Enhanced Removal of Pb 2+ From Aqueous Solution Using Modified Extracts From Food Processing Wastes: Design of Experiments

Eboseremen Sunday Okoebor
Department of Pure and Industrial Chemistry, University of Nigeria, Nsukka - Nigeria
Ikechukwu Daniel Anyaogu
Department of Science Laboratory Technology, Federal Polytechnic Nassarawa, Nassarawa State
Mathew Chukwudi Menkiti
Department of Chemical Engineering, Nnamdi Azikiwe University Awka, Anambra State Nigeria
Paul Madus Ejikeme (paul.ejikeme@unn.edu.ng)
Department of Pure and Industrial Chemistry, University of Nigeria, Nsukka - Nigeria

Research Article

Keywords: Central Composite Design, Response Surface Methodology, Scanning Electron Microscopy, ANOVA, Chitosan, Biosorption.

Posted Date: July 22nd, 2022

DOI: https://doi.org/10.21203/rs.3.rs-1843203/v1

Abstract

In this paper, biosorption of lead from aqueous solution on chitosan and modified chitosan from crab shells was investigated. Batch experiments have been carried out to find the effect of various parameters such as pH, temperature, sorbent dosage, heavy metal concentration and contact time on the biosorption of lead using these prepared adsorbents. Response surface methodology (RSM) was employed to optimize the process parameters. Based on the central composite design, quadratic model was developed to correlate the process variables to the response. The most influential factor on each experimental design response was identified from the analysis of variance (ANOVA). The optimum conditions for the biosorption of lead were found to be as follows: pH:10, temperature: 55°C, sorbent dosage: 2 g, metal concentration: 50 mg/L and contact time: 150 min. At these optimized conditions the maximum removal of lead by the chitosan and modified chitosan were found to be 84.38% and 89.83% respectively. From the analysis, the model's coefficient of determination (R^2) of (0.84 and 0.87 respectively of chitosan and modified chitosan) and F-value of (14.01 and 17.25 respectively for chitosan and modified chitosan) obtained proved that the experimental design model is adequate and can be used to navigate the design space. The sorbents were characterized using Fourier Transform Infra-red (FTIR) spectroscopy, Scanning Electron Microscopy (SEM), Differential Scanning Calorimetry (DSC) and X-Ray Diffraction (XRD) spectroscopy. Freundlich and Lineweaver-Burk isotherm model well expressed lead biosorption onto the studied sorbent. The metal biosorption onto the sorbents correlated well with pseudo-second-order kinetic model.

1. Introduction

Saving the environment and making the future of mankind safe is the timely focus. Lead is one of the most widely used non-ferrous metals in the electroplating industry, metallurgical industry, metal finishing industries, tannery operations, chemical manufacturing, mine drainage and battery manufacturing [1], [2]. Its presence in the environment is responsible for causing several damages to the ecosystem and adverse effects on public health. Residues of lead in the environment is particularly persistent in nature, highly toxic, nonbiodegradable, and accumulates in the food chain [3], [4]. Consequently, there is increasing attention on the removal and recovery of lead from various waste streams. Traditional methods such as chemical precipitation, evaporation, electroplating, adsorption and ion exchange processes have been used to remove lead from wastewater [5]–[10]. However, these technologies are most suitable in situations where the concentrations of the heavy metal ions are relatively high. They are either ineffective or expensive when heavy metals are present in the wastewater in low concentrations[11]. Therefore, new technologies are required to reduce heavy metal concentrations to environmentally acceptable levels at affordable costs.

Biological approaches, especially application of sorbents, have been suggested in the last decade. The advantages of sorbents are higher metal load capacity and greater selectivity for transition and heavy metals [11]–[13]. Marine food processing wastes have been found to be potential suitable sorbents because of their cheap availability, relatively high surface area and high binding affinity. The use of

chitosan for heavy metal removal has been reported by several authors; Nomanbhay and Palanisamy 2005, Isa *et al*., 2014, and Dotto *et al*., 2012[14]–[16]. Chitosan (poly-β-(1→4)-2-amino-2-deoxy-D-glucose) is a nitrogenous polysaccharide (amino-based) (see Fig. 2c) gotten by N-deacetylation of chitin(poly-β-(1→4)-N-acetyl-D-glucosamine) in large quantities. Chitin could be described as a natural biopolymer most bountifully found in marine media, particularly in crustacean exoskeletons, or cartilage of mollusk, micro-organisms' cell walls and cuticles of insects [17], [18]. The aim of the present investigation was to optimize the process parameters for the biosorption of lead on the modified chitosan using response surface methodology. RSM is a set of statistical procedures for planning experiments, constructing models, assessing the effects of variables, and determining the best conditions. It is commonly utilized for multivariable optimization studies in a variety of biotechnological processes, including media optimization, process conditions optimization, production optimization, fermentation optimization, metal biosorption optimization, and food processing optimization, among others [19]. In RSM, several factors are simultaneously varied.

2. Materials And Methods

All the chemicals used in this study were of analytical grade, purchased from Sigma Aldrich and used without any further purification.

2.1. Sample Collection and Pretreatment

Crab shells were collected from *Ishiet* in *Uruan* Local Government Area of Akwa Ibom State, Nigeria where they are readily available. The shells were washed properly with clean water, then rinsed with distilled water and dried. The dried crab shells were pulvirised using a high-power electric blender and sieved to obtain 250μm particle size for chitosan extraction [20].

2.2. Preparation of Adsorbent Material

The adsorbent was prepared following the method already reported by Okoya *et al*, [20]. The pulverized crab shells (200 g) was deproteinized using1:4 (W: V) of 4% (w/v) KOH at 80°C of constant stirring for 6 h. The residue was washed with distilled water until it was free of base and then dried at 100°C for 2 h. The resulting product was demineralized using 1: 2 (W: V) of 3% (v/v) HCl on a magnetic stirrer for 3 h at 30°C. Then filtered and the residue washed until it was free of acid. The acid free residue was then dried at 90°C for 1 h. A snow-white residue called chitin was obtained. Deacetylation was carried out on the chitin, using 50% (w/v) NaOH solution at 30°C with constant stirring for 4 h to obtain chitosan which washed and dried at 90°C for 1h.

2.3. Modification of Adsorbent

100ml of 1M solution of $H_3PO_4$was added to 100g of the extracted chitosan and the mixture was allowed to stand for 30mins, then the liquid discarded. The wet chitosan was spread on a stainless-steel tray and dried at 50°Cin a force air oven for 24h, then the temperature was raised to 180°Cfor 90mins.The

resulting chitosan was collected and allowed to cool before being washed in hot deionized water (60–80℃) and tested for free phosphate before being dried at 50℃ for 24 hours. This was done by combining 15ml of 20mM lead nitrate solution buffered to pH 4.8 in 0.03M acetic acid and 0.07M sodium acetate buffered with the filtrate, which did not turn cloudy.

2.4. Preparation of Pb(II) Stock Solution

Standard solution of Pb(II) was prepared from its nitrate salts. The working solution was prepared from stock solution containing 1000 mg/L of Pb (II). A pH meter (WTM VARIO) was utilized for pH measurement and the pH of the solution was adjusted to the desired value using0.1 M HCl and 0.1 M NaOH.

2.5. Design of Experiments (DOE) by RSM

In this study, the adsorption influencing parameters; contact time, pH, adsorbent dosage, temperature, and adsorbate concentration were coded as A, B, C, D and E respectively. A full factorial design, which includes all possible factor combinations in each of the factors, is a powerful tool for understanding complex processes for describing factor interactions in multifactor systems. RSM is an empirical statistical technique employed for multiple regression analysis by using quantitative data obtained from properly designed experiments to solve multivariate equations simultaneously[21]. Experiments with different pH, adsorbent dosages, temperatures, initial metal concentrations and processing time were carried out simultaneously covering the spectrum of variables for the removal of lead in the central composite design. To describe the effects of pH, adsorbent dosage, temperature, initial lead concentration and contact time on percentage removal of lead, batch experiments were conducted. The coded values of the process parameters were determined by the following equation:

{x}_{i}=\frac{{X}_{i}-{X}_{o}}{{\varDelta x}_{i}}
1

Where{x}_{i}is the coded value of the i^{th} variable, {X}_{i}is the uncoded value of the i^{th} test variable, {X}_{o}represents the uncoded value of the i^{th} test variable at the centre point, and{\varDelta x}_{i}defines the value of step change

According to the central composite design, for each variable, a 2^5 full factorial CCD for the five variables consisting of 32factorial points, 10axial points and 8replicates at the centre points was used[22]. However, a total of 50 experiments were necessary to find out the optimum preparation conditions and can be calculated from Eq. (2).

N=2n+{2}^{n}+c={2}^{5}+8=50
2

Where N is the total number of experiments required, n denotes the number of factors or variables, and c is the number of replicates.

The order of the experiments was randomised to diminish the effects of uncontrolled factors. Replicates at the central points were used to assess the residual error. The independent variables were coded to the (-1, 1) interval. The low and high levels are denoted by -1 and + 1, respectively. The axial points were located at (0, 0, ±\alpha), (0, ±\alpha, 0) and (±\alpha, 0, 0). Here, \alpha is the distance of the axial point from center. Table 1 depicts the ranges and the levels of the influencing factors studied. The empirical model was developed for each response which correlated the response with five influencing variables by applying a second degree polynomial equation [21]. This can be represented as follows:

Y={b}_{0}+\sum _{i}^{n}=1{b}_{i}{x}_{i}+{\left(\sum _{i}^{n}=1{b}_{ii}{x}_{i}\right)}^{2}+{\sum }_{i-1}^{n-1}{\sum }_{j=i+1}^{n-1}={b}_{ij}{x}_{i}{x}_{ij}

3

Where Y represents the predicted response, $b_0$isthe constant coefficient, {b}_{i}denotes the linear coefficients, {b}_{ij }isthe interaction coefficients, {b}_{ii}definesthe quadratic coefficients respectively, {x}_{i}, and {x}_{ij}arethe coded values of the prepared adsorbent influencing variables.

Table1: Independent variables and their coded levels for the CCD coded

Variables	Code	Units	Coded Variable levels				
			$-\alpha$	-1	0	$+1$	$+\alpha$
Time	A	min	5	5	77.5	150	150
pH	B		2	2	6	10	10
Dosage	C	g	0.5	0.5	1.25	2	2
Temperature	D	℃	25	25	40	55	55
Initial Conc.	E	mg/L	50	50	125	200	200

2.6. Batch Adsorption Experiments

The batch experiments performed with variations of the process factors including contact time (5-150 min), adsorbent dosage (0.5-2.0 g), pH (2–10), temperature (25-55^{o}C) and initial metal ion concentration (50–200 mg/L) were analyzed using the central composite design (CCD)[23]. The 50 experimental runs with the various combinations of the different factors were randomly performed to determine the best condition for the chitosan and modified chitosan according to Table 2, by mechanical agitation.

Table 2

Design Matrix and Responses from Chitosan and modified chitosan in the bisorption of Pb^{2+}

Runs	A	B	C	D	E	Lead Removal (%)	
	Time (mins)	pH	Dosage (g)	Temp. (°C)	Conc. (mg/L)	Modified Chitosan	chitosan
1	150	10	0.5	25	50	86.11	74.99
2	5	10	2	55	200	66.02	12.94
3	77.5	6	1.25	40	125	61.06	58.40
4	5	10	0.5	25	50	58.2	22.74
5	5	2	2	55	200	53.36	65.85
6	77.5	6	1.25	40	125	66.53	34.75
7	5	10	2	25	50	79.46	49.48
8	150	2	0.5	25	200	64.78	74.60
9	5	2	2	55	50	67.24	54.98
10	150	10	2	25	200	84.72	50.38
11	150	10	2	25	50	69.42	39.85
12	5	2	2	25	50	59.03	22.84
13	150	10	0.5	25	200	78.76	20.43
14	5	2	0.5	55	200	56.65	50.88
15	77.5	6	2	40	125	64.49	18.56
16	150	10	0.5	55	50	88.19	20.50
17	5	10	2	25	200	55.20	50.83
18	77.5	6	1.25	55	125	68.40	35.69
19	77.5	6	1.25	40	125	69.22	40.48
20	77.5	6	1.25	40	125	74.41	44.89
21	77.5	6	0.53	40	125	69.60	45.29
22	5	10	0.5	25	200	78.72	49.79
23	150	10	0.5	55	200	61.81	30.32
24	150	2	2	55	200	77.01	13.20
25	77.5	6	1.25	40	125	74.41	11.50

Runs	A	B	C	D	E	Lead Removal (%)	
	Time (mins)	pH	Dosage (g)	Temp. (°C)	Conc. (mg/L)	Modified Chitosan	chitosan
26	5	10	2	55	50	74.21	8.49
27	77.5	10	1.25	40	125	62.44	32.98
28	150	2	1.625	25	50	57.74	31.39
29	77.5	6	1.25	40	125	71.28	29.48
30	5	10	0.5	55	200	79.86	25.47
31	77.5	6	1.25	40	200	72.93	11.84
32	5	2	0.5	25	200	55.72	56.85
33	77.5	6	1.25	40	125	69.93	59.38
34	77.5	6	1.25	40	125	57.32	45.48
35	77.5	6	1.25	40	125	75.36	26.38
36	77.5	6	1.25	40	125	70.01	22.38
37	5	2	2	25	200	54.81	44.89
38	150	2	2	55	50	54.44	30.25
39	150	2	0.5	25	50	58.20	71.10
40	150	10	2	55	200	81.33	69.68
41	5	2	0.5	55	50	64.21	65.79
42	5	2	0.5	25	50	63.68	22.89
43	77.5	6	1.25	40	200	69.60	81.87
44	150	10	2	55	50	89.83	84.38
45	150	2	0.5	55	50	60.45	9.48
46	150	2	0.5	55	200	49.66	19.39
47	150	2	2	25	200	62.83	49.33
48	5	10	0.5	55	50	41.03	22.48
49	77.5	6	1.25	40	125	74.47	49.58
50	77.5	6	1.25	40	125	70.01	7.56

Key: A = time(mins), B = pH, C = Dosage (g), D = Temp. E = Adsorbate Conc. (mg/L).

A known mass of adsorbent was added to each, 20mL solution of lead (II) ions of known pH and known initial metal ion concentration. After agitation, the solution was filtered using a Whatman110mm filter paper and the residual Pb^{2+}in the filtrate was analyzed by AAS. The amount of Pb^{2+} ions adsorbed at equilibrium (q_e) and the removal efficiency (E) were calculated using the following equation.

{q}_{e}=\frac{V\left({C}_{0}-{C}_{e}\right)}{W}
4
E=\frac{\left({C}_{0}-{C}_{e}\right)}{{C}_{0}}\times 100
5
Where q_e is the amount of adsorbate adsorbed per unit mass of chitosan or its modified derivative at equilibrium measured in mg/g, C_0 and C_e are the initial and equilibrium concentrations of metal ions respectively in mg/L, V is the volume of adsorbate solution in litres and W is the mass of adsorbent in grams.

2.7. Adsorption Equilibrium and Kinetic Studies

Adsorption isotherms and kinetic models are usually used to explore the interactions between the adsorbent and adsorbate at equilibrium and to establish the mechanism of the adsorption process. To find the most appropriate isotherm and kinetic model for the adsorption of lead from aqueous solution, Langmuir [24],Freundlich[25],Temkin[26], Dubinin–Radushkevich [27], [28], and Lineweaver-Burk isotherms [29]were used to analyse the results. The kinetics of the sorption process was studied with the Pseudo- First Order Kinetic Model(Farouq and Yousef 2015), Pseudo-Second Order (Farouq and Yousef 2015), Elovich kinetic [31], Bhattacharya and Venkobachar Kinetic Model [32], Weber-Morris intra-particle diffusion Model [33], and Film Diffusion Model[34]. For both equilibrium and kinetic studies, the adsorption experiments were done at predetermined time intervals for lead concentration analysis using optimized conditions obtained previously from the CCD analysis. The equations for isotherms and kinetic models explored in this study are presented in Table 3.

3. Results And Discussion

3.1. Characterization

3.1.1 Fourier Transform Infrared Spectra Analysis

The Fourier transform infrared spectrum of the chitosan and the modified chitosan before adsorption is given in Fig. 1a and 1b respectively. From Fig. 1a, it can be observed from that the functional groups responsible for the adsorption on the surface of the adsorbent are the hydroxyl group and amino group at 3427cm^{-1}. The peaks observed at 3072, 2911, and 2734 cm^{-1} were assigned to the stretching vibrations of C–H bond in methyl group while 1383 cm^{-1} could be associated to the bending vibration of C–H bond in the methyl group and the band at 878 cm-1 can represents the symmetrical vibration in a chain of P-O-P and to P-C phosphorus-containing compound as seen in the figure. These functional groups are

negatively charged and can attract positively charged lead metal ions. While Fig. 1b, it can be observed that the functional groups responsible for adsorption on the surface of the adsorbent are, a hydroxyl group and amino group at 3427 cm^{-1}region.The peaks observed at 3072, 2911 and 2734 cm^{-1} were assigned to the stretching vibrations of C–H bond in methyl group while 1383 cm^{-1} was assigned to the bending vibration of C–H bond in methyl group[35].

From Fig. 2a and 2b, the decrease in the number of peaks after adsorption, formation of new absorption bands, the change in absorption intensity, and the shift in wavenumber of functional groups could be attributed to complexation between metal ions and binding sites of adsorbents. The binding mechanism involved sharing of electron pair between electron donor atoms (O and N) and metal ion. FTIR suggests that both hydroxyl and amine groups are indeed the main adsorption sites in the chitosan and the modified chitosan(Kyzas and Bikiaris 2015).

Table 3
Kinetics and Isotherm Models Equations Explored

Kinetic Models	Equations	Isotherm Models	Equations
Pseudo- First Order	\frac{{d}_{qt}}{dt}= {K}_{1}\left({q}_{e}-{q}_{t}\right)	Langmuir	\frac{{C}_{e}}{{q}_{e}}=\frac{1}{{K}_{L}{q}_{m}}+\frac{{C}_{e}}{{q}_{e}}
Pseudo-Second Order	\frac{dqt}{dt}= {K}_{2}{\left({q}_{e}-{q}_{t}\right)}^{2}	Freundlich	\text{log}{q}_{e}=\text{log}K+\frac{1}{n} \times \text{log}{C}_{e}
Elovich	\left(\frac{dqt}{dt}\right)=a\text{exp}\left(-bqt\right)	Temkin	{q}_{e} = Bln{A}_{T} + Bln{C}_{e}
Bhattacharya and Venkobachar	\text{ln}\left(1-Ut\right)=-\beta t	Dubinin–Radushkevich	ln{q}_{e}= ln{q}_{o}- $K_d\varepsilon^2$
Weber and Morris	{q}_{t} = K_{id} $t^{1/2}$ + C	Lineweaver-Burk	\frac{1}{{q}_{e}}= \frac{1}{{q}_{m}}+ \frac{1}{{q}_{m}{K}_{L}{C}_{e}}
Boyd Model	Log({q}_{m}– {q}_{t}) = log({q}_{m}) –\left(\frac{{D}_{i}}{2.303}\right)		

3.1.2. Scanning Electron Microscope (SEM)

Figures 3a, 3b, 4a and 4b show that the investigated adsorbent contains many pores in which metal ions can be trapped and adsorbed. Because of its uniform surface area, the material's shape can enhance metal adsorption[20]. Furthermore, SEM analysis revealed the significant changes on the surface morphology after modification with phosphoric acid as shown by Fig. 4a. The surface of the phosphoric acid modified chitosan is rougher than that of the chitosan. So based on the morphology, it can be concluded that this material presents an adequate morphological profile to retain metal ions.

3.1.3. X-ray Diffraction (XRD) Analysis

XRD patterns for the chitosan and modified chitosan are shown in Figs. 5a and 5b. The obtained characteristic diffraction peaks for these biosorbents are consistent with those in the literature (Kyzas and Deliyanni, 2013; Balau et al., 2004). In the X–ray diffraction spectrogram of chitosan, a broad peak at 2θ = 20.2° present due to the amorphous state of chitosan with other three characteristic peaks at 20.6°, 20.9° and 30.4° attributable to the indices were observed. In the spectrogram for the phosphoric acid modified chitosan, only a broad peak at 2θ = 20° was observed. The average crystallite size, D (nm), ofthe modified chitosan was calculated about 10.5 nm, using the Debye–Scherrer equation [37]:

$$D=\frac{{K}_{s}.{\lambda }}{B.cos{\theta }}$$

6

Where Ks is a constant (Ks = 0.9 for CuKa), λ (nm) is the wavelength (0.15405 nm for CuKa), B is the peak width of half–maximum (rad) and θ is the diffraction angle.

Phosphoric acid reduces the crystallinity of the raw chitosan and improves it via cross linking, thereby making modified chitosan less crystalline as confirmed by XRD analysis[39]. Crystallinity lowers adsorption capacity because there is less surface area and few open active sites for metal binding compared to amorphous adsorbents with large surface area and more open active sites. This reduction in crystallinity enhances the probability for an adsorbate to interact with the adsorbent due to loosen inter-chain structure and bonding, thus expose more active sites for adsorption which increased the adsorption capacity of the modified chitosan [40].

3.1.4. Differential Scanning CalorimetryThermogram

The thermogram for the chitosan and the modified chitosan are given in Fig. 6a and 6b respectively. From Fig. 6a, a broad endotherm over the temperature range of 28 and 98°C (with peak at 83.42°C) was seen, followed by a sharp endotherm which peaked at 204.71°C. The diffuse endotherm of chitosan which peaked at 83.42°C can be ascribed to loss of the absorbed water (Dhawade and Jagtap 2012; Jana et al., 2015)and 0.009824J of heat per milligram sample of the adsorbent was absorbed in the process. The second endotherm can be ascribed to polymer melting. The area under the curve (0.0021143 J/mg) represents the latent heat of melting while the peak (204.71°C) represents the melting point of the polymer [41]. From Fig. 6b, the first endotherm of the modified chitosan corresponds to relaxation transition, which peaked at 193.81^{o}C. Endothermic relaxation is a second order reaction just like glass transition [43]. Meanwhile, second endotherm which can be attributed to polymer (phosphoric acid

modified chitosan) melting picked at 240^{o}C. It is obvious that the modified chitosan demonstrated significant stability over a wide temperature range (80-170^{o}C).

3.2. Development of Model Equation

The design matrix containing the studied factors, their ranges and the response which is the removal efficiency (%) of Pb(II), (Y_{pmc}) and ({\mathbf{Y}}_{\mathbf{c}\mathbf{s}}) is presented in Table 2. The results obtained were then evaluated with CCD in RSM for the development of the model's regression equation. A quadratic second order polynomial expression as suggested by the software fitted the data suitably. The model equation was selected in conformity with the sequential model sum of the square that is based on the highest order polynomial where the additional terms of the model are significant, and the model is not aliased. Both the regression coefficients (R^2) and adjusted R^2wereused to validate the quality of the proposed models; values closer to 1.0 confirm a good agreement between the predicted and experimental data. Thus, the correlation between experimental and predicted response is evident as indicated by the model's R^2 and adjusted R^2 values of 0.94 and 0.90, which were within the desirability range. The final model's equation for the removal efficiency of lead by modified chitosan, ({\mathbf{Y}}_{\mathbf{p}\mathbf{m}\mathbf{c}}) and raw chitosan, ({\mathbf{Y}}_{\mathbf{c}\mathbf{s}}) are given by Eqs. (7) and (8) respectively:

{\mathbf{Y}}_{\mathbf{p}\mathbf{m}\mathbf{c}} = 74.57829+6.1607035*A + 8.2275766*B + 2.3218341*C-0.104926*D + 0.2963844*E-3.320276*A^2-5.156986*B^2-2.437222*C^2-2.73161*D^2-0.116199*E^2 + 2.2462946*AB-1.761432*AC + 1.3925446*AD-2.74808*AE + 2.3489324*BC + 2.7949554*BD-0.14192*BE + 2.1239324*CD-0.725443*CE + 1.1368304*DE (7)

{\mathbf{Y}}_{\mathbf{c}\mathbf{s}} = 63.72168 + 6.603598*A + 7.481349*B -0.31528*C-1.61259D-0.36278*E-0.92096*A^2-4.42379*B^2-0.5086*C^2 + 1.594576*D^2-0.8856*E^2 + 2.963686*AB-0.95303*AC + 1.135561*AD-2.39256*AE + 1.960528*BC + 1.990689*BD-1.91994*BE + 1.752403*CD-0.00822*CE + 1.208189*DE (8)

The cooperative and counter effects of the studied factors were elucidated by the negative and positive coefficients before the terms in the model equation. A negative coefficient value implies that the term negatively affects Pb^{2+}adsorption (i.e. the removal efficiency decreases), whereas a positive coefficient values mean that the term increase Pb^{2+}adsorption in the tested range (Muluh, 2017).

Table 4

Statistical parameters obtained from the analysis of variances (ANOVA) for the

models for Pb (II) Ion % removal from waste water by the raw and modified chitosan.

Statistical Parameters	chitosan	Modified chitosan
Std. Dev.	4.95	4.88
Mean	59.32	62.72
Coefficient of variation, CV	8.34	7.78
PRESS	2684.98	2762.28
R- squared (R^2)	0.91	0.92
R^2 adjusted	0.84	0.87
Predicted R^2	0.77	0.69
Adequate Precision	19.39	19.90

Table 5a: Analysis of variances (ANOVA) and lack-of- fit test for response surface quadratic model for removal of Pb (II) ions from aqueous solution by the modified chitosan

Source	Sum of squares	DF	Mean square	F-Value	Prob.>F	Comment
Model	8209.80	20	410.49	17.25	< 0.0001	Significant
A	1641.90	1	1641.90	69.00	< 0.0001	
B	2928.41	1	2928.40	123.07	< 0.0001	
C	228.50	1	228.49	9.60	0.0043	
D	0.47	1	0.48	0.02	0.8885	
E	3.80	1	3.80	0.16	0.6923	
A2	612.18	1	612.18	25.73	< 0.0001	
B2	1476.80	1	1476.80	62.07	< 0.0001	
C2	330.25	1	330.24	13.88	0.0008	
D2	414.35	1	414.35	17.41	0.0002	
E2	0.75	1	0.75	0.03	0.8603	
AB	161.19	1	161.19	6.77	0.0144	
AC	96.43	1	96.43	4.05	0.0535	
AD	61.95	1	61.95	2.60	0.1174	
AE	241.26	1	241.26	10.13	0.0035	
BC	171.48	1	171.48	7.20	0.0119	
BD	249.56	1	249.56	10.49	0.0030	
BE	0.64	1	0.64	0.03	0.8705	
CD	140.20	1	140.19	5.89	0.0216	
CE	16.36	1	16.36	0.68	0.4138	
DE	41.29	1	41.29	1.74	0.1981	
Residual	690.00	29	23.79			
Lack of Fit	689.62	22	31.35	0.83	< 0.0001	Not significant
Pure Error	0.38	7	0.05			
Cor Total	8899.80	49				

Table 5b: Analysis of variances (ANOVA) and lack-of- fit test for response surface quadratic model for removal of Pb (II) ion from aqueous solution by the chitosan

Source	Sum of squares	DF	Mean square		F-Value	Prob.>F	Comment
Model	6852.60	20	342.63	14.01		< 0.0001	Significant
A	1886.46	1	1886.46	77.15		< 0.0001	
B	2421.29	1	2421.29	99.02		< 0.0001	
C	4.21	1	4.21	0.17		0.6811	
D	112.49	1	112.49	4.60		0.0405	
E	5.69	1	5.69	0.23		0.6331	
A2	47.09	1	47.09	1.93		0.1758	
B2	1086.72	1	1086.72	44.44		< 0.0001	
C2	14.38	1	14.38	0.59		0.4493	
D2	141.19	1	141.19	5.77		0.0229	
E2	43.55	1	43.55	1.78		0.1924	
AB	280.59	1	280.59	11.48		0.0020	
AC	28.23	1	28.23	1.15		0.2915	
AD	41.19	1	41.19	1.68		0.2045	
AE	182.87	1	182.87	7.48		0.0105	
BC	119.46	1	119.45	4.88		0.0351	
BD	126.59	1	126.59	5.18		0.0305	
BE	117.75	1	117.75	4.82		0.0364	
CD	95.44	1	95.44	3.90		0.0578	
CE	0.02	1	0.01	8.59		0.9927	
DE	46.63	1	46.63	1.90		0.1778	
Residual	709.13	29	24.45				
Lack of Fit	690.19	22	31.37	0.60		0.0014	Not significant
Pure Error	18.93	7	2.70				
Cor Total	7561.73	49					

3.3. Statistical Analysis

The fitness of the model was investigated using the analysis of variance (ANOVA) at 95% confidence interval. The ANOVA of Pb^{2+} removal efficiency by modified chitosan and chitosan are presented in Table 5a and 5b respectively. The significance and insignificance of each term in the model were determined by the Fisher's F-test and P-value. The model *F*-value of 17.25 and 14.01 respectively for modified chitosan and chitosan, which implies that the model is significant and the P-value is less than 0.05[23], [44]. A high value of the adjusted determination coefficient (R^2-Adj = 0.84 and 0.87 for chitosan and modified chitosan respectively) was estimated. This result means that 84% and 87% of the total variation on Pb(II) adsorption data can be described by the selected model. Based on the P-values presented in Table 5a, the significant model terms were A, B, C, D, E,B^2, D^2, E^2, AB, BC, BD, BE and CD with AC, AD, CE, DE, A^2, C^2 and E^2 insignificant to the response. In order to simplify the model Chitosan, the insignificant terms (AC, AD, CE, DE, A^2, C^2 and E^2) can be eliminated. And based on the P-values presented in Table 5b, the significant model terms were A, B, C, D, E, A^2, B^2, C^2, D^2, E^2, AB, BC, BD, BE and CD with AC, AD, CE and DE insignificant to the response. In order to simplify the model for modified chitosan, the insignificant terms (AC, AD, CE and DE) can be eliminated. Adequate precision (AP) is basically a measure of signal to noise ratio. Ratios greater than 4 indicate that the model is adequate and can be used to navigate the design space[23], [44]. In this study, the AP ratio of 19.39 and 19.90 respectively of chitosan and modified chitosan, indicate an adequate signal and thus the model can be used to predict the responses. The coefficient of variation (CV) is the ratio of the standard deviation of the mean expressed as a percentage. For a model to be considered reliable and reproducible, it must have a CV less than 10% [23]. In this investigation, the CV value of 8.34% and 7.78% respectively of chitosan and modified chitosan reflect a good precision and reliability of the experiments.

3.4. Effects of individual variables and their interactions

It can be inferred from Tables 2, 5a and 5b that the individual effects of factors (contact time, pH, adsorbent dose and initial concentration) on lead uptake by chitosan and modified chitosan were more dominant than the effect of temperature, based on their high F-values of 0.23 and 0.16 (initial concentration), 0.17 and 9.60 (adsorbent dose), 99.09 and 123.08 (pH), 77.15 and 69.01 (contact time) and 4.60 and 0.02 (temperature) respectively of the prepared adsorbents. The two factor interaction effects of initial concentration and pH (F-value of 3.36 and 12.28), initial concentration and contact time (40.70 and 5.64) respectively of the prepared adsorbent are more pronounced in the interaction. From these results, it can be concluded that the adsorption of lead from aqueous solution by chitosan and phosphoric acid modified chitosan is highly dependent on initial concentration of adsorbate and the combined effects of the contact time or pH and initial concentration of adsorbate, due to their very high F-values. Figure 7 to 9 depicts the three-dimensional response surfaces of the interaction effects of the process variables on the adsorption of lead and can be noticed that an increase in the removal efficiency of Pb (II) by prepared chitosan and the modified chitosan can be observed with decrease in initial concentration, increase in the mass of adsorbent, in the contact time and increase in pH to a maximum of about 10. The interaction effect of initial concentration and pH can be observed to show a lopsided effect on Lead removal efficiency.

3.5. Adsorption Isotherm Studies

Adsorption isotherms are useful in determining the nature of the interaction between the adsorbate and the adsorbent. To determine the most befitting isotherm model for the sorption of lead, the equilibrium data obtained using optimized values for the studied parameters were fitted to the Langmuir, Freundlich, Temkins, Dubinin-Radushkevich and Lineweaver-Burk isotherm models. The results of the isotherm parameters from the plots are presented in Table 6, and Freundlich isotherm model (Fig. 10) with coefficient of determination (R^2 = 0.9286 and 0.9323 for chitosan and modified chitosan respectively) and Lineweaver-Burk isotherm model (Fig. 11) with coefficient of determination (R^2 = 0.9518 and 0.9664 respectively for chitosan and modified chitosan) appeared to be much more relevant in fitting the experimental data than the other models studied.

The fitness of the Freundlich model implies that the adsorption of Pb^{2+} ions from bulk solution assumes heterogeneous surface energies. It can be observed from Table 6 that the n values gotten from the Freundlich plot were greater than unity for the studied concentration range; this suggests that the adsorption conditions were favourable. All the R_L (dimensionless separation factor) values from the Langmuir plot lie between 0 and 1 indicating that the adsorption process is favourable for the under studied conditions [45]

Table 6: Adsorption isotherm parameters for different models studied

Isotherm Models	Modified chitosan	Chitosan
Langmuir model		
q_m (mg/g)	2.600	0.2413
K_L	0.0374	0.0248
R^2	0.7801	0.6660
R_L	0.3484	0.4462
Freundlich model		
N	1.718	1.701
K_f	0.166	0.154
R^2	0.9323	0.9286
Temkin model		
(Lmg^{-1})	0.423	0.370
B	0.496	0.407
R^2	0.8021	0.7969
Dubinin-Radushkevich model		
(mg/g)	1.224	1.153
E ($KJmol^{-1}$)	176776.7	176776.7
$(mol^2KJ^{-2})10^{-6}$	$4\ 10^{-6}$	$4\ 10^{-6}$
R^2	0.7909	0.7791
Lineweaver-Burk		
R^2	0.9664	0.9518
q_m (mg/g)	2.600	0.2413

3.6. Adsorption Kinetic Studies

Four linearized forms of kinetic models viz; pseudo-first order, pseudo-second order, Elovich kinetic model, Bhattacharya and Venkobachar kinetic model and Weber and Morris intra-particle diffusion kinetic models have been used to analyze the collected experimental data and the linear plots obtained for the different kinetic models are presented in Fig. 15to20 with the kinetic parameters and coefficients of

determination values obtained summarized in Table 7. The pseudo-second-order kinetics model fitted well to the adsorption data as observed from the high R^2 value ($R^2 > 0.99$). More so, it best predicted the value for q_e than those of first-order model given in Table 7.Therefore, it can be stated that the rate-controlling step is chemisorption, involving valence forces through sharing or exchange of electrons between the adsorbent surface and adsorbate ions with no involvement of a mass transfer in solution[46]. A deviation of plot from origin was seen in the intra-particle diffusion model indicating that it is not the sole rate-limiting step of the reaction. This deviation from the origin could be because of difference in the rate of mass transfer in the initial and final step of the adsorption process [47]. The C (mg g^{-1}) values of the intra-particle diffusion model indicate the boundary layer thickness of Pb^{2+} on the adsorbent surface. The C values from the parameters were observed to be smaller than the experimental q_e values (Table 7) and this means that Pb^{2+} uptake on these adsorbents involved both surface adsorption and partitioning inside adsorbent components such organic matter and aliphatic amino groups, among other things.

Table 7: Summary of parameters for kinetic models studied

Kinetic Models	Modified chitosan	Chitosan
Pseudo-first order		
K_1 (Min^{-1})	0.0106	0.0092
R_1^2	0.909	0.811
q_e(mg/g)	0.181	0.177
Pseudo-second order		
K_2 (mg/g min)	0.339	0.379
R_2^2	0.9937	0.9839
q_e cal. (mg/g)	0.423	0.382
Elovich		
R^2	0.9695	0.8236
B	27.03	30.49
(ab)	1.172	1.183
Bhattacharya and Venkobachar		
R^2	0.8941	0.7863
β	0.011	0.009
Weber and Morris		
K_{id}(mg/g min)	0.014	0.011
C	0.246	0.233
R^2	0.9365	0.8909
Boyd model		
Intercept	-0.8534	-0.914
Di (cm^2/s)	-0.0111	-0.0062
R^2	0.9102	0.8866

3.5. Process Optimization/Validation

The function of desirability with preparation conditions was applied. Based on economical perspective of production process, the variables were set within the studied range and goals were targeted to achieve maximum possible removal percentage by the software. The optimum condition chosen by the software was: Contact time, pH, Adsorbent dose, Temperature and Adsorbate initial concentration of 150min, 10, 2.0g, 55°C, and 50mg/L respectively to obtain highest removal efficiency. At this optimum condition, removal percentage obtained by chitosan and the modified chitosan biosorbents were 84 and 87% respectively. The experimental values obtained were in good agreement with the predicted results by the software with relatively small errors of 0.38 and 2.83% respectively. A plot of studentized residuals versus run order was tested and the residuals were scattered randomly around ± 3sigma (Fig. 21). This was an indication of better fit for both the models with the experimental data and shows that the model fits well to optimize the independent variables for the removal of Pb(II)[44].

Conclusion

This article focuses on lead (II) ion adsorption onto chitosan and phosphoric acid modified chitosan from aqueous solution. Response surface methodology based on CCD model was used to determine the optimum reaction conditions. According to the ANOVA analysis, all the interaction terms are statistically significant. The quadratic model represented adequately the response surface area based on the adjusted determination coefficient (R2Adj = 0.84 and 0.87 respectively for chitosan and modified chitosan) and the adequate precision ratio (19.39 and 19.90 respectively for chitosan and modified chitosan). The high similarity between the experimental value and the predicted values suggested that the model was a good fit. The results of from study revealed that chitosan have predominantly adsorptive capacity which could be enhanced through modification, (especially chemical modification). The adsorption capacity of the chitosan and phosphoric acid modified chitosan for Pb2+ increased with increase in pH, concentrations, contact time and temperature. Furthermore, the values of the adsorption capacities obtained in the study were indicative of the affinity of lead to the studied adsorbents

Declarations

Ethics approval and consent to participate: No human / animal study requiring approval involved in the study.

Consent for publication: All authors consent sought before sending manuscript for review.

Availability of data and materials: No data available

Competing interests: No competing interest exists.

Funding: No funding to be declared.

Authors' contributions: OES carried-out the laboratory work and jointly wrote the manuscript with IDA; PME and MMC designed the work and reviewed the manuscript.

Acknowledgements: The Department of Pure and Industrial Chemistry, University of Nigeria is acknowledged for providing the enabling environment for the work to be done.

Authors' information (optional) -
If any of the sections are not relevant to your manuscript, please include the heading and write 'Not applicable' for that section.

Low resolution image identified during revised manuscript technical check, please replace images with a higher resolution image (300 DPI or better) if possible: Attempt has been made to obtain high resolution images.

Kindly provide the corresponding author's email address in the title page of the manuscript: The email has been provided.

References

1. R. K. Gautam, A. Mudhoo, G. Lofrano, and M. C. Chattopadhyaya, “Biomass-derived biosorbents for metal ions sequestration: Adsorbent modification and activation methods and adsorbent regeneration,” J. Environ. Chem. Eng., vol. 2, no. 1, pp. 239–259, 2014, doi: 10.1016/j.jece.2013.12.019.
2. V. Chandra, I. Deo, and I. Mani, “Adsorption thermodynamics and isosteric heat of adsorption of toxic metal ions onto bagasse fly ash (BFA) and rice husk ash (RHA),” vol. 132, pp. 267–278, 2007, doi: 10.1016/j.cej.2007.01.007.
3. H. Olumayowa Oluwasola *et al.*, “Geochemical and health risk assessment of heavy metals concentration in soils around Oke-Ere mining area in Kogi State, Nigeria,” Int. J. Environ. Anal. Chem., pp. 1–16, Jan. 2021, doi: 10.1080/03067319.2020.1862817.
4. S. Chowdhury, R. Mishra, P. Saha, and P. Kushwaha, “Adsorption thermodynamics, kinetics and isosteric heat of adsorption of malachite green onto chemically modified rice husk,” Desalination, vol. 265, no. 1–3, pp. 159–168, 2011, doi: 10.1016/j.desal.2010.07.047.
5. M. K. David, U. C. Okoro, K. G. Akpomie, C. Okey, and H. O. Oluwasola, “Thermal and hydrothermal alkaline modification of kaolin for the adsorptive removal of lead(II) ions from aqueous solution,” SN Appl. Sci., vol. 2, no. 6, Jun. 2020, doi: 10.1007/s42452-020-2621-7.
6. A. Khatri, M. H. Peerzada, M. Mohsin, and M. White, “A review on developments in dyeing cotton fabrics with reactive dyes for reducing effluent pollution,” J. Clean. Prod., vol. 87, no. 1, pp. 50–57, 2015, doi: 10.1016/j.jclepro.2014.09.017.
7. J. Hu, X. Yang, L. Shao, X. He, and K. Men, “Effect of alkali treatment on heavy metals adsorption capacity of sewage sludge,” in *International Conference on Environmental Pollution and Public*

Health, EPPH 2015, 2015, pp. 33–39. doi: 10.4236/gep.2015.32006.

8. T. K. Sen and C. Khoo, “Adsorption Characteristics of Zinc (Zn 2+) from Aqueous Solution by Natural Bentonite and Kaolin Clay Minerals: A Comparative Study,” *Comput. Water, Energy, Environ. Eng.*, vol. 2, no. July, pp. 1–6, 2013, doi: 10.4236/cweee.2013.23B001.
9. O. E. Abdel, N. A. Reiad, and M. M. Elshafei, “A study of the removal characteristics of heavy metals from wastewater by low-cost adsorbents,” J. Adv. Res., vol. 2, no. 4, pp. 297–303, 2011, doi: 10.1016/j.jare.2011.01.008.
10. M. A. Barakat, “New trends in removing heavy metals from industrial wastewater,” Arabian Journal of Chemistry, vol. 4, no. 4. pp. 361–377, Oct. 2011. doi: 10.1016/j.arabjc.2010.07.019.
11. M. B. Desta, “Batch sorption experiments: Langmuir and freundlich isotherm studies for the adsorption of textile metal ions onto teff straw (eragrostis tef) agricultural waste,” J. Thermodyn., vol. 1, no. 1, 2013, doi: 10.1155/2013/375830.
12. A. M. Mohammad, T. A. Salah Eldin, M. A. Hassan, and B. E. El-Anadouli, “Efficient treatment of lead-containing wastewater by hydroxyapatite/chitosan nanostructures,” Arab. J. Chem., 2014, doi: 10.1016/j.arabjc.2014.12.016.
13. M. Parmar and L. S. Thakur, “Review article HEAVY METAL CU, NI AND ZN : TOXICITY, HEALTH HAZARDS AND THEIR REMOVAL TECHNIQUES BY LOW COST ADSORBENTS : A SHORT OVERVIEW 1 M. Tech Research Scholar, Department of Chemical Engineering, Ujjain Engineering College, Ujjain – 456010 ,),” pp. 143–157, 2013.
14. S. M. Nomanbhay and K. Palanisamy, “Removal of heavy metal from industrial wastewater using chitosan coated oil palm shell charcoal,” Electron. J. Biotechnol., vol. 8, no. 1, pp. 43–53, 2005, doi: 10.2225/vol8-issue1-fulltext-7.
15. M. T. Isa, A. Abdulkarim, J. A. Muhammad, A. O. Ameh, and S. Abdulsalam, “Kinetic and Thermodynamic Studies of Chromium Ion Adsorption Using Chitosan from Mussel Shell,” vol. 21, pp. 43–52, 2014.
16. G. L. Dotto, M. L. G. Vieira, and L. A. A. Pinto, “Kinetics and Mechanism of Tartrazine Adsorption onto Chitin and Chitosan,” 2012.
17. G. Z. Kyzas and D. N. Bikiaris, “Recent Modifications of Chitosan for Adsorption Applications:,” pp. 312–337, 2015, doi: 10.3390/md13010312.
18. Z. Limam, S. Selmi, S. Sadok, and A. El Abed, “Extraction and characterization of chitin and chitosan from crustacean by-products: Biological and physicochemical properties,” African J. Biotechnol., vol. 10, no. 4, pp. 640–647, 2013, doi: 10.4314/ajb.v10i4.
19. M. Rajasimman and K. Murugaiyan, “Sorption of Nickel by Hypnea Valentiae: Application of Response Surface Methodology,” Jan. 2011, doi: 10.5281/ZENODO.1085589.
20. A. A. Okoya, A. B. Akinyele, I. E. Ofoezie, O. S. Amuda, O. S. Alayande, and O. W. Makinde, “Adsorption of heavy metal ions onto chitosan grafted cocoa husk char,” vol. 8, no. 10, pp. 147–161, 2014, doi: 10.5897/AJPAC2014.0591.

21. Z. Z. Chowdhury, S. M. Zain, R. A. Khan, A. A. Ahmad, and K. Khalid, “Application of Response Surface Methodology (RSM) for Optimizing Production Condition for Removal of Pb (II) and Cu (II) Onto Kenaf Fiber Based Activated Carbon,” vol. 4, no. 5, pp. 458–465, 2012.
22. U. Managamuri, M. Vijayalakshmi, S. Poda, V. S. R. K. Ganduri, and R. S. Babu, “Optimization of culture conditions by response surface methodology and unstructured kinetic modeling for bioactive metabolite production by Nocardiopsis litoralis VSM-8,” *3 Biotech*, vol. 6, no. 2, pp. 1–19, 2016, doi: 10.1007/s13205-016-0535-2.
23. N. S. Muluh, “Central composite design analysis and optimization of cadmium adsorption from synthetic wastewater by avocado seed activated carbon,” vol. 2, no. 5, pp. 652–661, 2017.
24. B. Salunkhe and S. J. Raut, “Removal of heavy metal Ni (II) and Cr (VI) from aqueous solution by scolecite natural zeolite,” Int. J. Chem. Sci., vol. 10, no. 2, pp. 1133–1148, 2012.
25. A. Proctor and J. F. Toro-Vazquez, “The Freundlich Isotherm in Studying Adsorption in Oil Processing,” Bleach. Purifying Fats Oils Theory Pract., pp. 209–219, Mar. 2009, doi: 10.1016/B978-1-893997-91-2.50016-X.
26. R. Farouq and N. S. Yousef, “Equilibrium and Kinetics Studies of adsorption of Copper (II) Ions on Natural Biosorbent,” *Int. J. Chem. Eng. Appl.*, vol. 6, no. 5, pp. 319–324, Oct. 2015, doi: 10.7763/IJCEA.2015.V6.503.
27. Q. Hu and Z. Zhang, “Application of Dubinin–Radushkevich isotherm model at the solid/solution interface: A theoretical analysis,” *J. Mol. Liq.*, vol. 277, pp. 646–648, Mar. 2019, doi: 10.1016/J.MOLLIQ.2019.01.005.
28. D. Balarak, F. K. Mostafapour, and H. Azarpira, “Langmuir, Freundlich, Temkin and Dubinin – radushkevich Isotherms Studies of Equilibrium Sorption of Ampicilin unto Montmorillonite Nanoparticles,” vol. 20, no. 2, pp. 1–9, 2017, doi: 10.9734/JPRI/2017/38056.
29. M. Benjelloun, Y. Miyah, G. Akdemir Evrendilek, F. Zerrouq, and S. Lairini, “Recent Advances in Adsorption Kinetic Models: Their Application to Dye Types,” Arab. J. Chem., vol. 14, no. 4, p. 103031, Apr. 2021, doi: 10.1016/J.ARABJC.2021.103031.
30. R. Farouq and N. S. Yousef, “Equilibrium and Kinetics Studies of adsorption of Copper (II) Ions on Natural Biosorbent,” vol. 6, no. 5, 2015, doi: 10.7763/IJCEA.2015.V6.503.
31. F. C. Wu, R. L. Tseng, and R. S. Juang, “Characteristics of Elovich equation used for the analysis of adsorption kinetics in dye-chitosan systems,” *Chem. Eng. J.*, vol. 150, no. 2–3, pp. 366–373, Aug. 2009, doi: 10.1016/J.CEJ.2009.01.014.
32. T. Michalev and I. Petrov, “The Removal of Heavy Metal Ions by Synthetic Zeolites: A Review,” pp. 79–84, 2012.
33. P. Veetil NIDHEESH, R. Gandhimathi, S. Thanga RAMESH, and T. Sarasvathy ANANTHA SINGH, “Kinetic analysis of crystal violet adsorption on to bottom ash,” Turkish J. Eng. Env. Sci, vol. 36, pp. 249–262, 2012, doi: 10.3906/muh-1110-3.
34. Y. S. Ho, J. C. Y. Ng, and G. Mckay, “KINETICS OF POLLUTANT SORPTION BY BIOSORBENTS: REVIEW,” vol. 29, no. 2, pp. 189–232, 2000.

35. M. F. Queiroz, K. R. T. Melo, D. A. Sabry, G. L. Sassaki, and H. A. O. Rocha, “Does the use of chitosan contribute to oxalate kidney stone formation?,” Mar. Drugs, vol. 13, no. 1, pp. 141–158, 2015, doi: 10.3390/md13010141.
36. G. Z. Kyzas and D. N. Bikiaris, “Recent modifications of chitosan for adsorption applications: A critical and systematic review,” Mar. Drugs, vol. 13, no. 1, pp. 312–337, 2015, doi: 10.3390/md13010312.
37. G. Z. Kyzas and E. A. Deliyanni, “Mercury(II) removal with modified magnetic chitosan adsorbents,” Molecules, vol. 18, no. 6, pp. 6193–6214, 2013, doi: 10.3390/molecules18066193.
38. L. Balau, G. Lisa, M. I. Popa, V. Tura, and V. Melnig, “Physico – chemical properties of Chitosan films,” vol. 2, no. 4, pp. 638–647, 2004.
39. M. D. Ries and L. Pruitt, “Effect of cross-linking on the microstructure and mechanical properties of ultra-high molecular weight polyethylene,” Clin. Orthop. Relat. Res., vol. 440, no. 440, pp. 149–156, 2005, doi: 10.1097/01.blo.0000185310.59202.e5.
40. V. V. Pchelintsev, A. Y. Sokolov, and G. E. Zaikov, “Effect of chemical structure and crystallinity on sorption, diffusion and chemical stability of polyurethaneacetals,” Polym. Degrad. Stab., vol. 19, no. 2, pp. 125–134, Jan. 1987, doi: 10.1016/0141-3910(87)90071-1.
41. P. P. Dhawade and R. N. Jagtap, “Characterization of the glass transition temperature of chitosan and its oligomers by temperature modulated differential scanning calorimetry,” vol. 3, no. 3, pp. 1372–1382, 2012.
42. S. Jana *et al.*, “Pharmaceutica Analytica Acta Characterization of Physicochemical and Thermal Properties of Chitosan and Sodium Alginate after Biofield Treatment,” vol. 6, no. 10, 2015, doi: 10.4172/21532435.1000430.
43. E. O. Olorunsola, O. J. Olayemi, S. O. Majekodunmi, and U. B. Etukudo, “Extraction and physicochemical characterization of a potential multifunctional pharma-excipient from crab shell wastes,” vol. 14, no. 40, pp. 2856–2861, 2015, doi: 10.5897/AJB2015.14819.
44. B. Sadhukhan, N. K. Mondal, and S. Chattoraj, “Optimisation using central composite design (CCD) and the desirability function for sorption of methylene blue from aqueous solution onto Lemna major,” Karbala Int. J. Mod. Sci., vol. 2, no. 3, pp. 145–155, Sep. 2016, doi: 10.1016/J.KIJOMS.2016.03.005.
45. J.-H. Park *et al.*, “Competitive adsorption and selectivity sequence of heavy metals by chicken bone-derived biochar: Batch and column experiment,” *J. Environ. Sci. Heal. Part A*, vol. 50, no. 11, pp. 1194–1204, Sep. 2015, doi: 10.1080/10934529.2015.1047680.
46. M. Arshadi, M. J. Amiri, and S. Mousavi, “Kinetic, equilibrium and thermodynamic investigations of Ni(II), Cd(II), Cu(II) and Co(II) adsorption on barley straw ash,” Water Resour. Ind., vol. 6, pp. 1–17, 2014, doi: 10.1016/j.wri.2014.06.001.
47. I. A. W. Tan and B. H. Hameed, “Adsorption isotherms, kinetics, thermodynamics and desorption studies of basic dye on activated carbon derived from oil palm empty fruit bunch,” J. Appl. Sci., vol. 10, no. 21, pp. 2565–2571, 2010, doi: 10.3923/jas.2010.2565.2571.

Figures

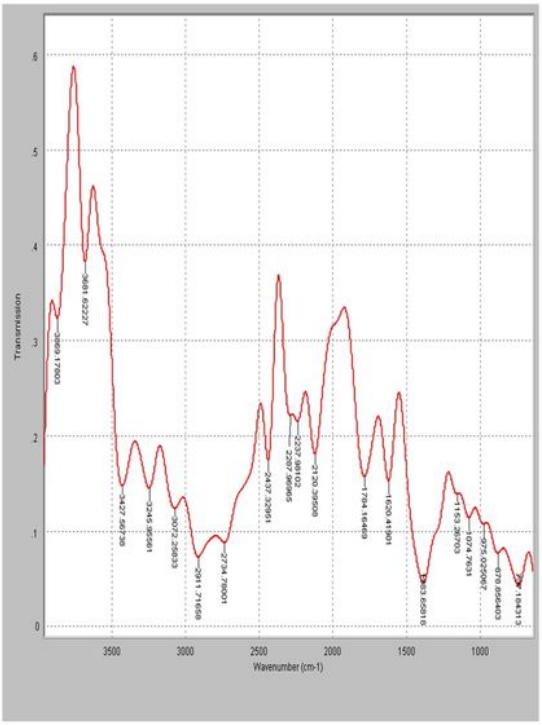

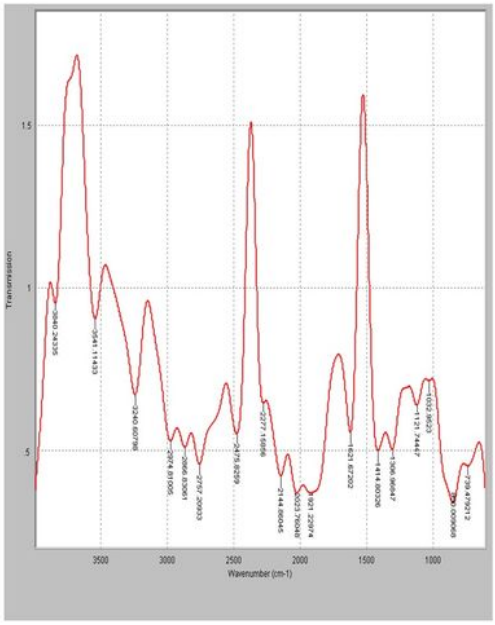

Figure 1

a: Fourier transform infrared spectrum of chitosan before pb^{2+} adsorption

b: Fourier transform infrared spectrum of modified chitosan before Pb^{2+} adsorption

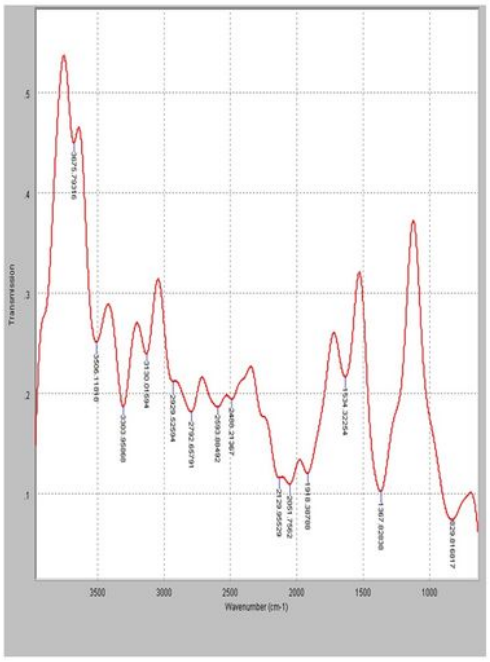

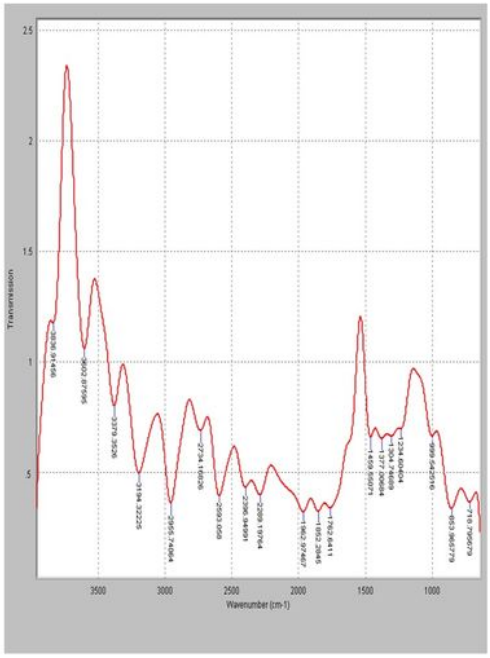

Figure 2

a: Fourier transform infrared spectrum of chitosan after Pb^{2+} adsorption

b: Fourier transform infrared spectrum of modified chitosan after Pb^{2+} adsorption

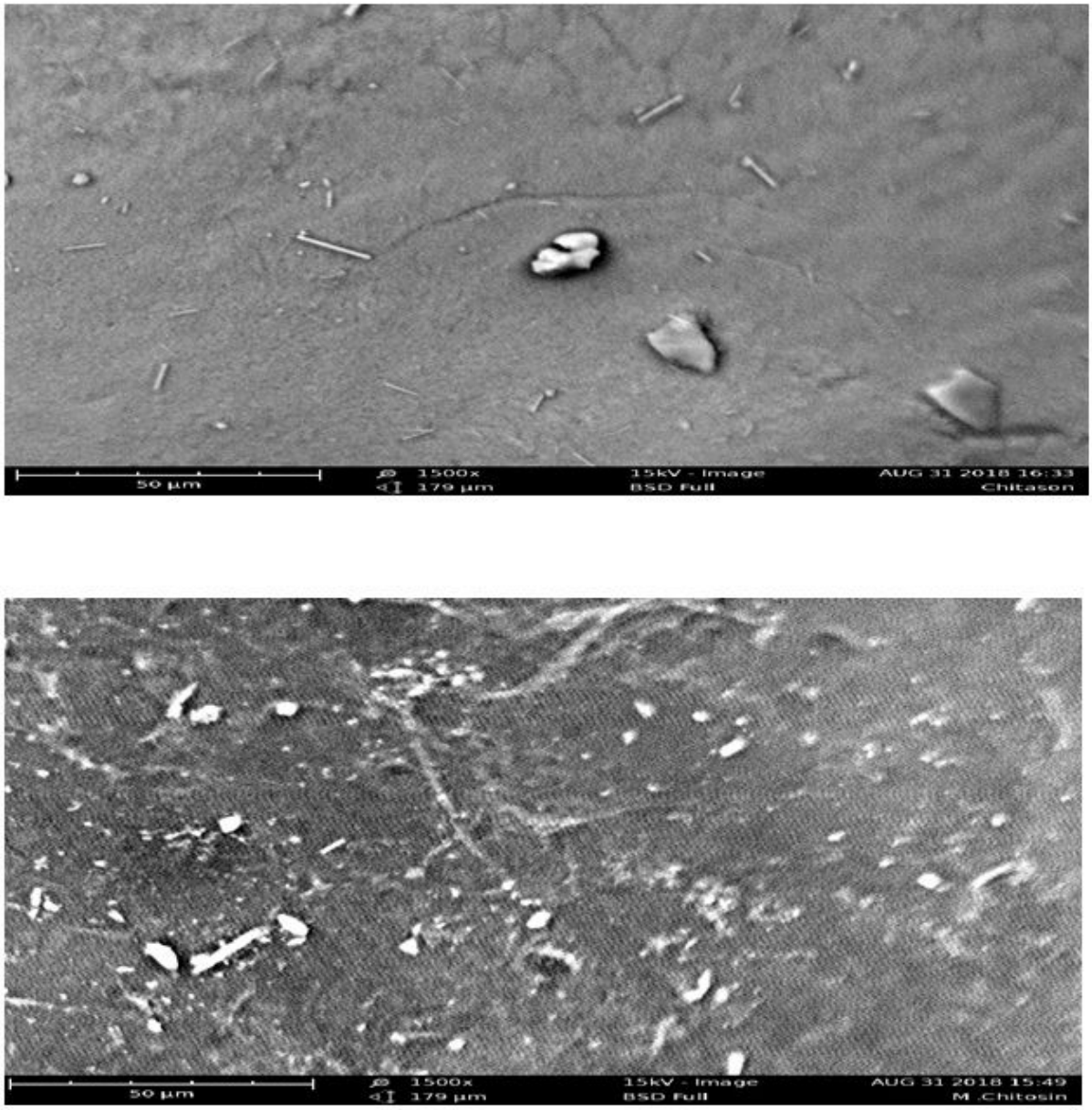

Figure 3

a: SEM for chitosan before pb^{2+} adsorption

b.SEM for modified chitosan before Pb^{2+} adsorption

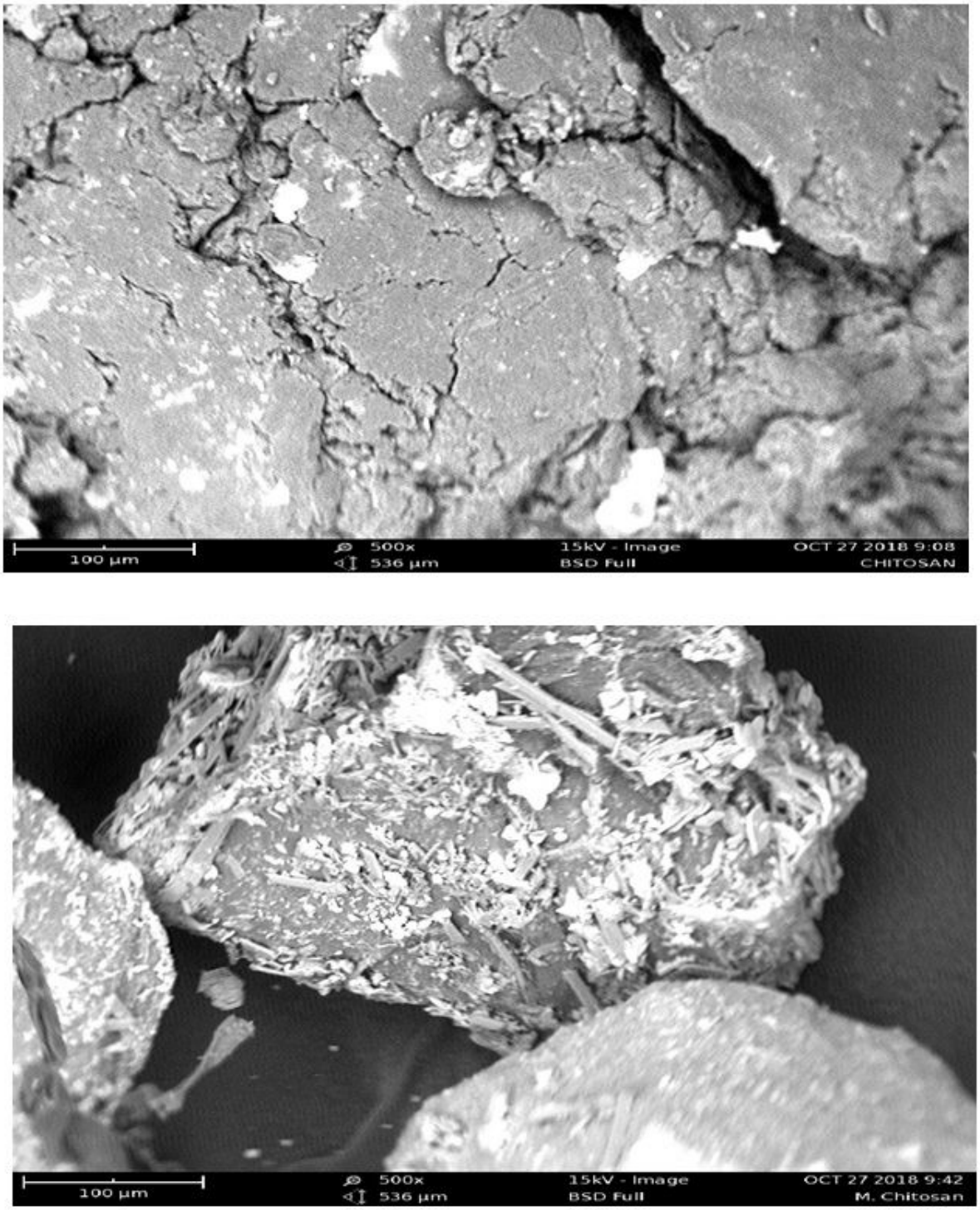

Figure 4

a: SEM for chitosan after Pb^{2+} adsorption.

b: SEM for modified chitosan after Pb^{2+} adsorption

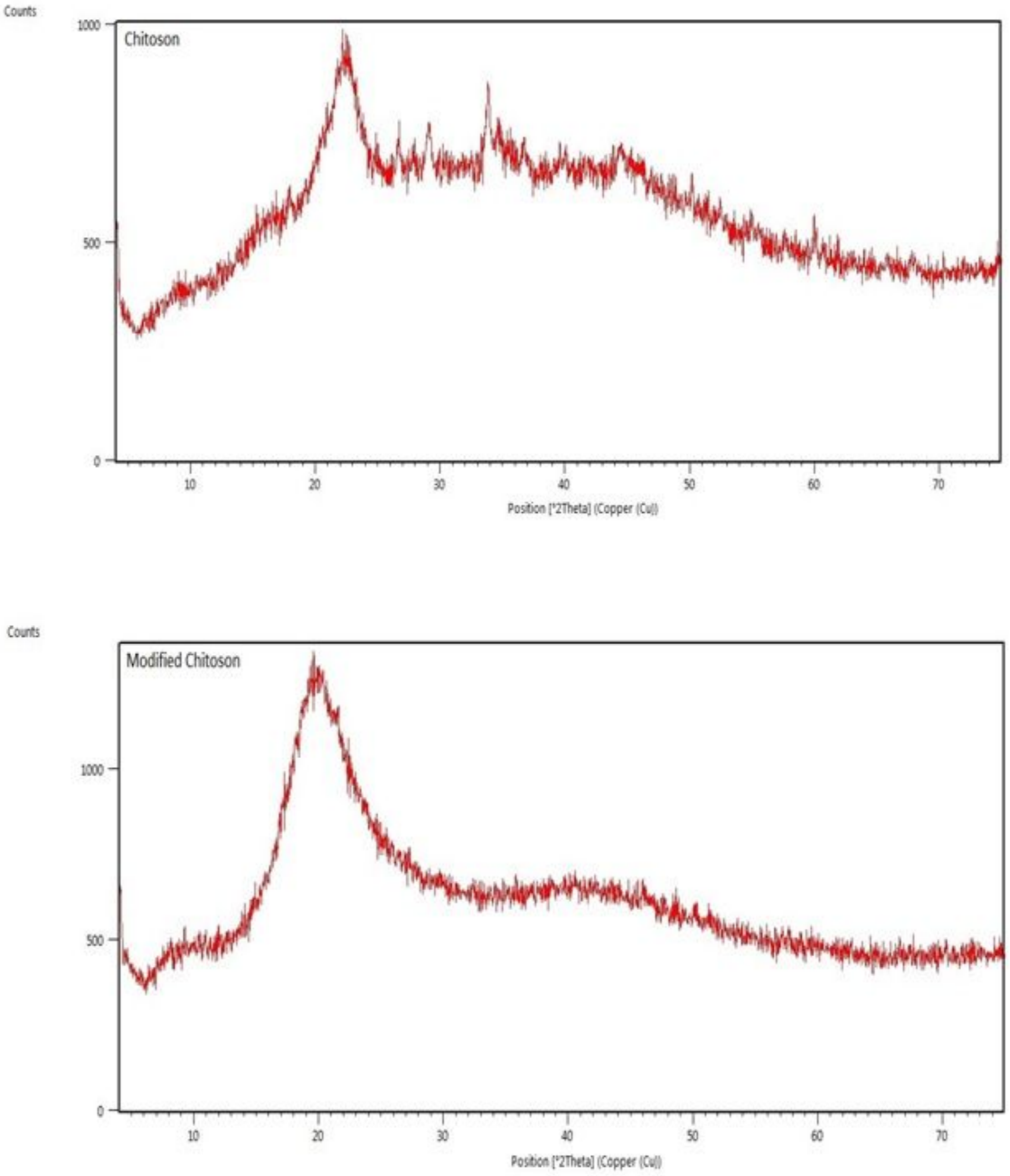

Figure 5

a: XRD patterns for the chitosan

b: XRD patterns for the modified chitosan

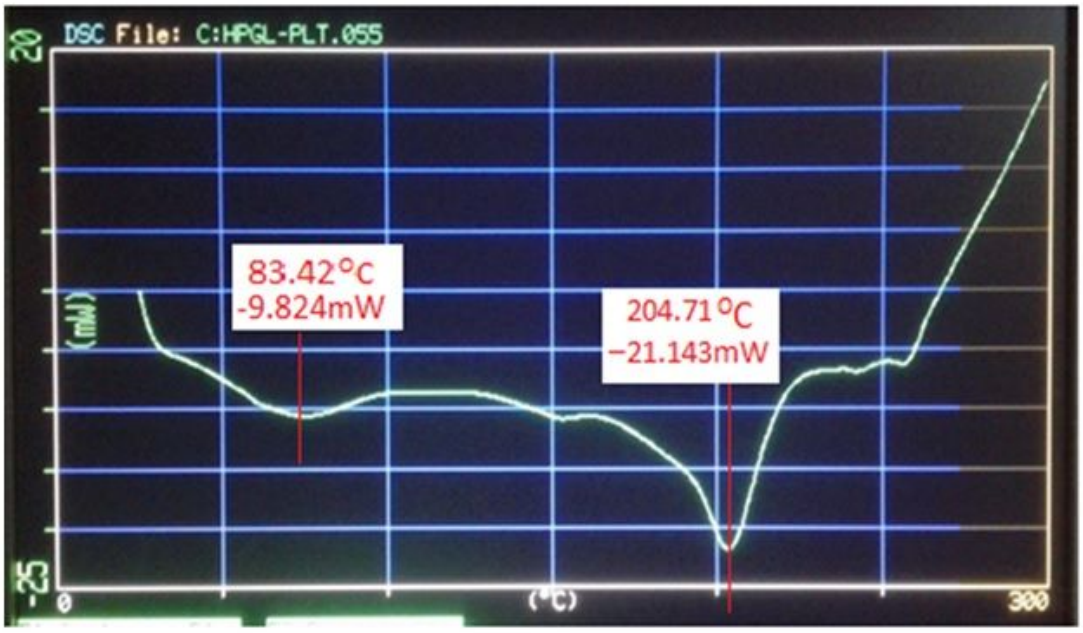

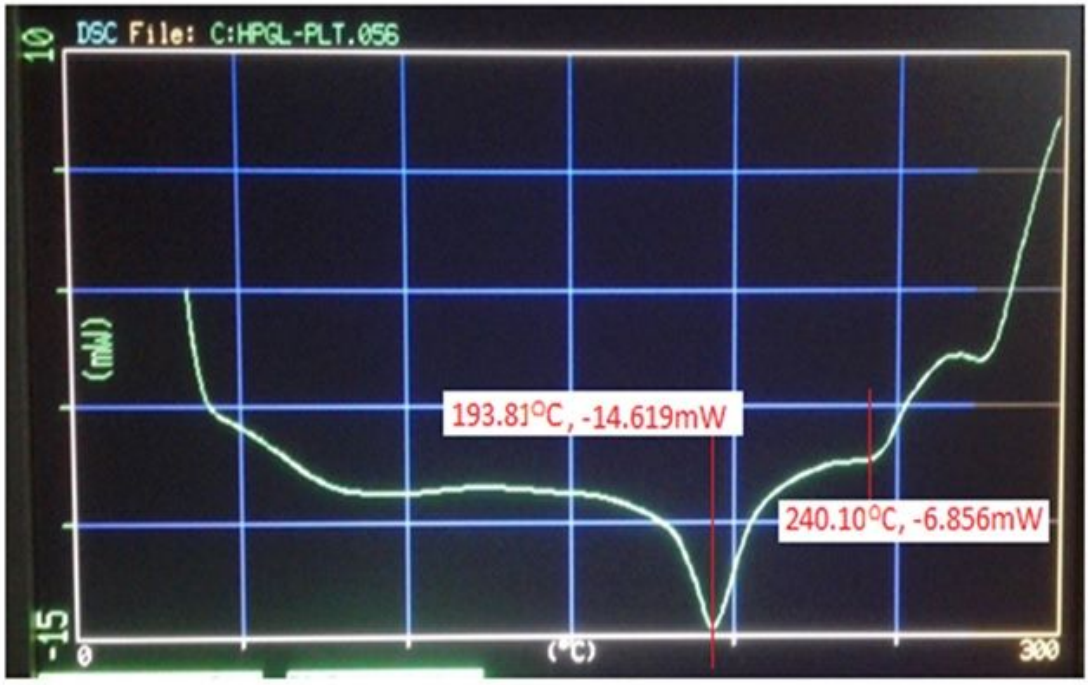

Figure 6

a:DSC Thermogram of the Chitosan

b.DSC thermogram of the modified chitosan

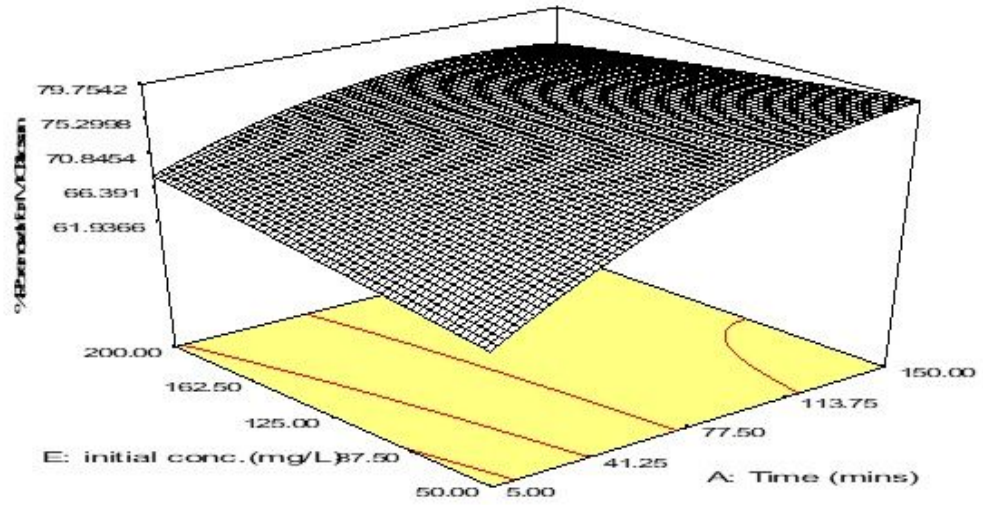

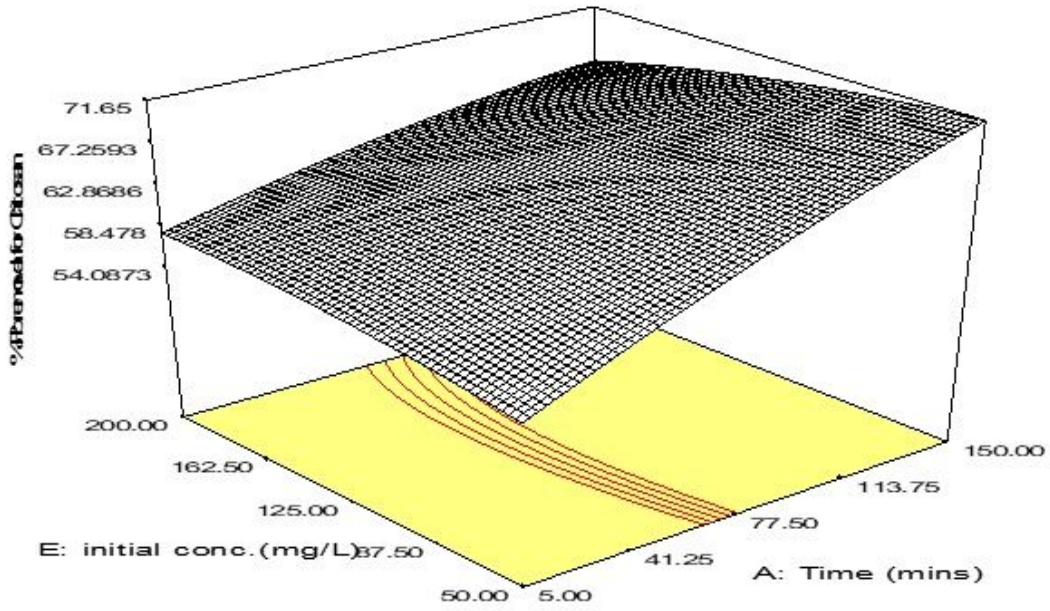

Figure 7

3D Response surface plots of interaction effects of initial concentration and time for the adsorption of lead by modified chitosan

3D Response surface plots of interaction effects of initial concentration and time for the adsorption of lead byprepared raw chitosan

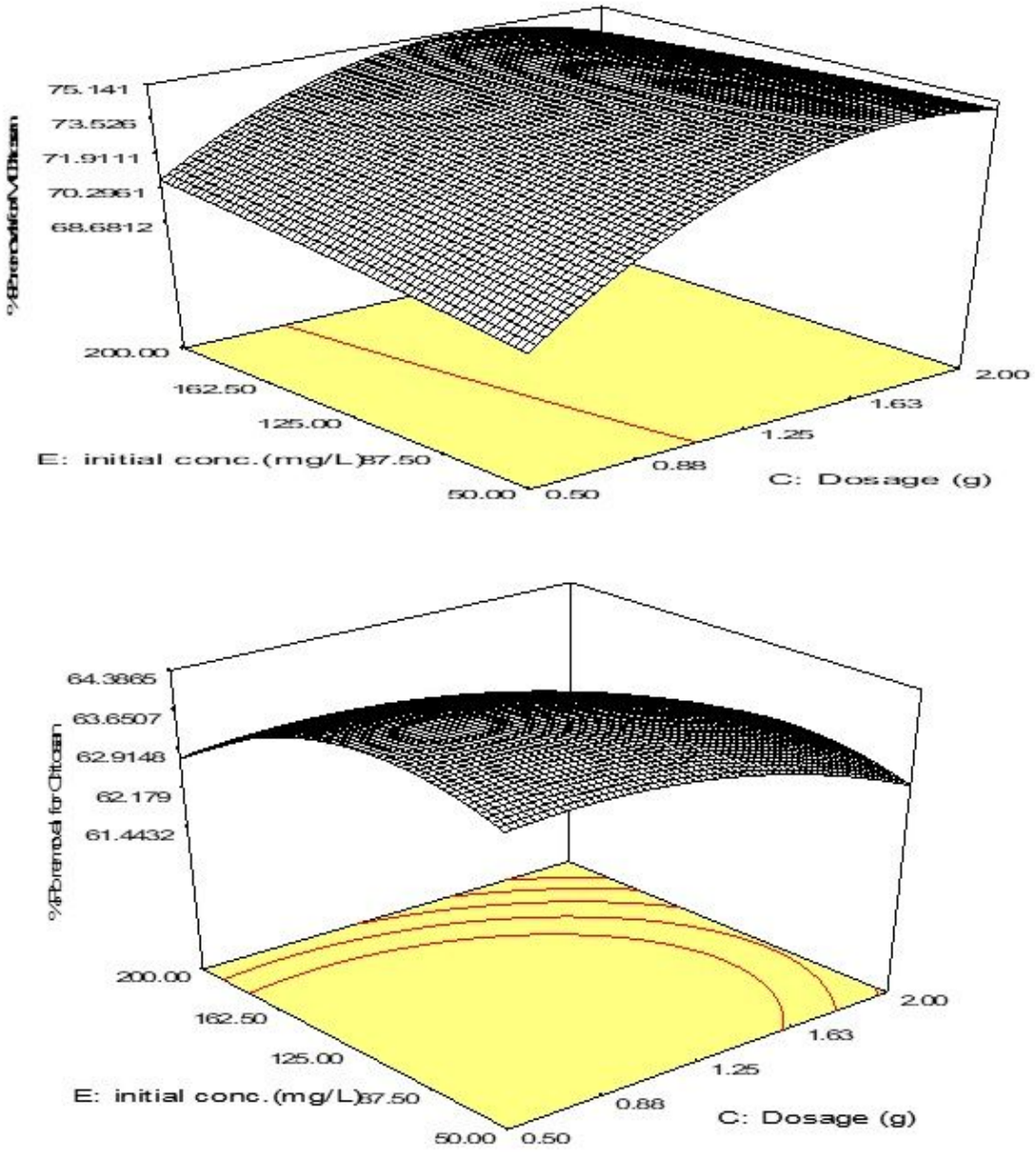

Figure 8

3D Response surface plots of interaction effects of initial concentration and adsorbent dosage and for the adsorption of lead bymodified chitosan.

3D Response surface plots of interaction effects of initial concentration and dosage for the adsorption of lead by the prepared raw chitosan

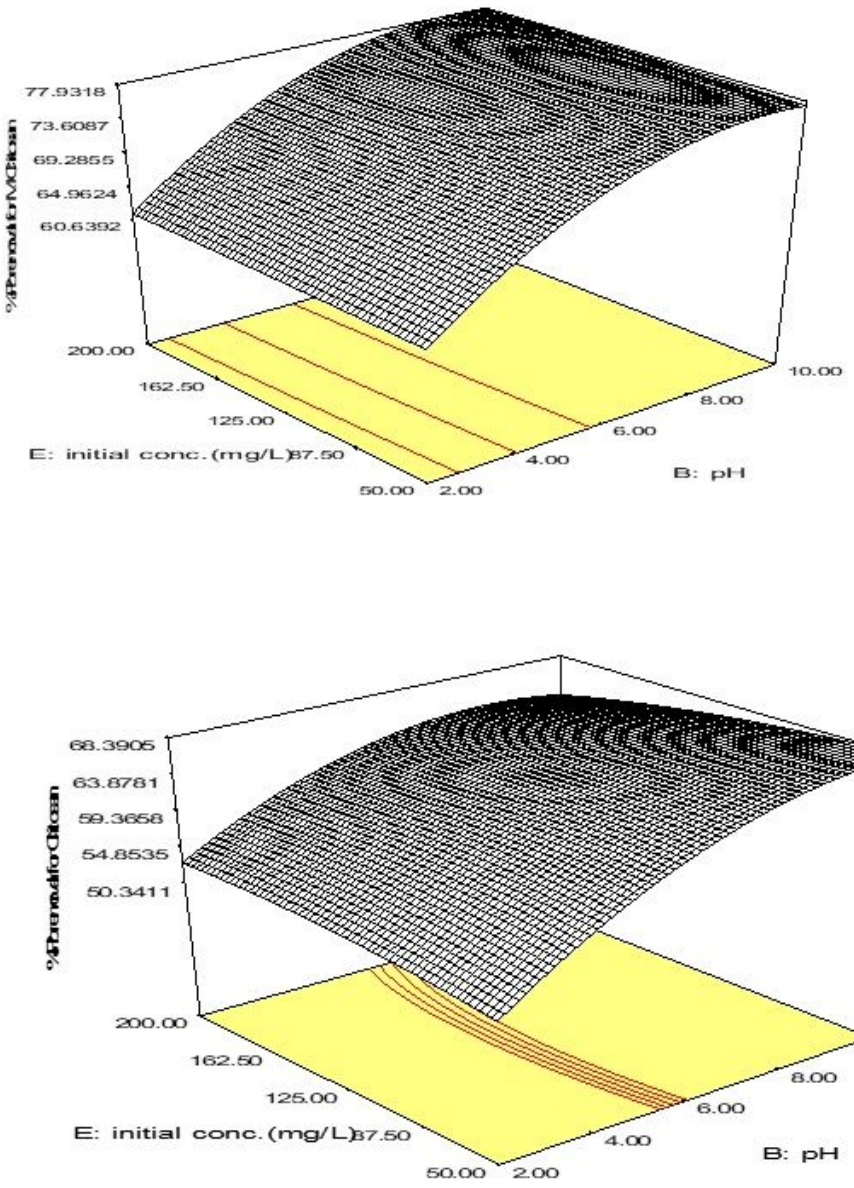

Figure 9

3D Response surface plots of interaction effects of initial concentration and pH for the adsorption of lead bymodified chitosan.

3D Response surface plots of interaction effects of initial concentration and pH for the adsorption of lead bythe prepared raw chitosan

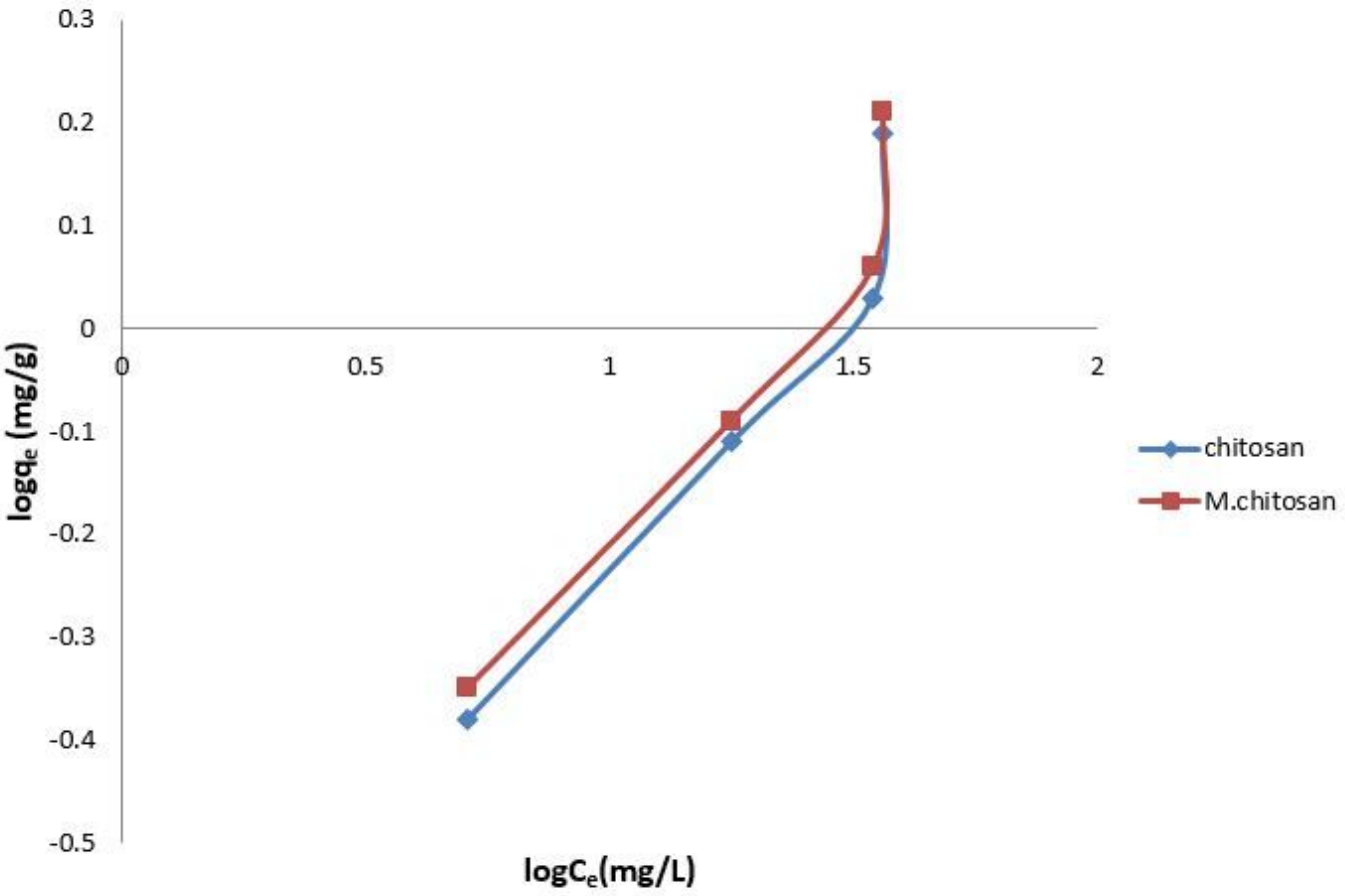

Figure 10

A plot of Freundlich isotherm of Pb^{2+}adsorption by extracted modified chitosan

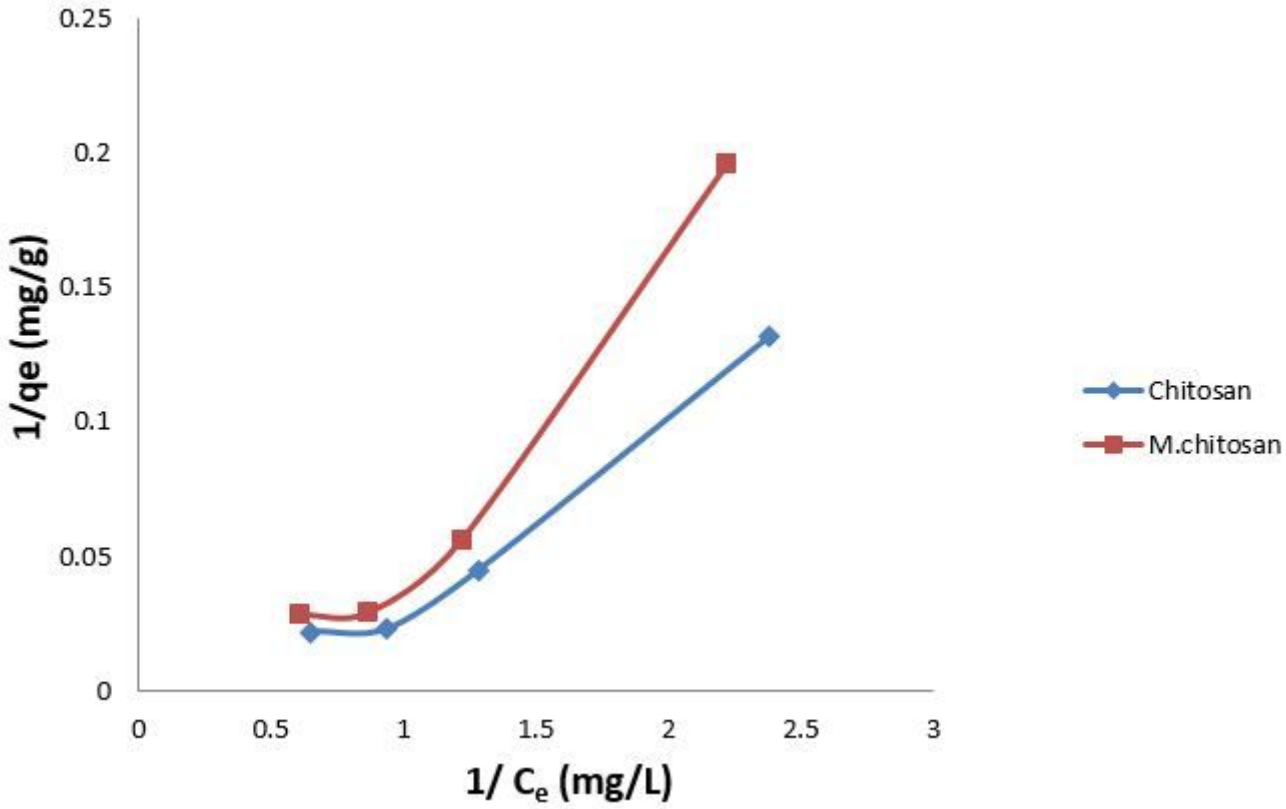

Figure 11

A plot of Lineweaver-Burk Isotherm of Pb^{2+} adsorption by chitosan and modified chitosan

Image not available with this version

Figure 12

This image is not available with this version.

Image not available with this version

Figure 13

This image is not available with this version.

Image not available with this version

Figure 14

This image is not available with this version.

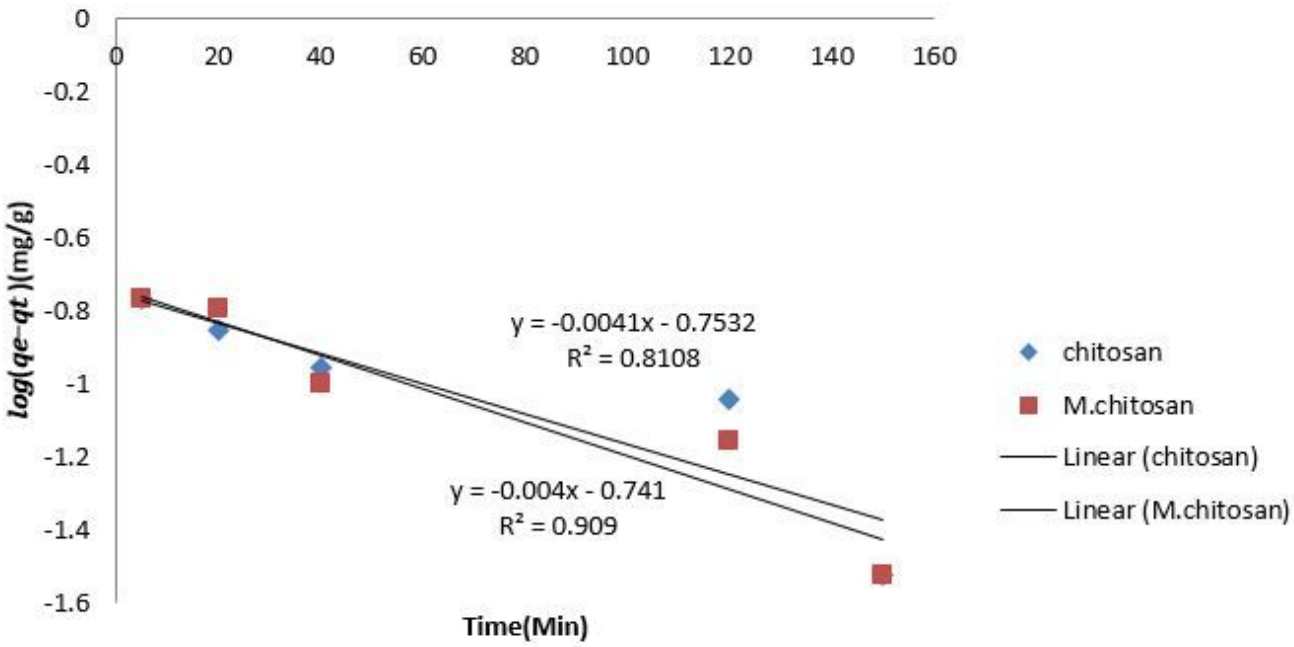

Figure 15

Plot of pseudo-first order kinetics for Pb^{2+} adsorption by extracted chitosan and modified chitosan

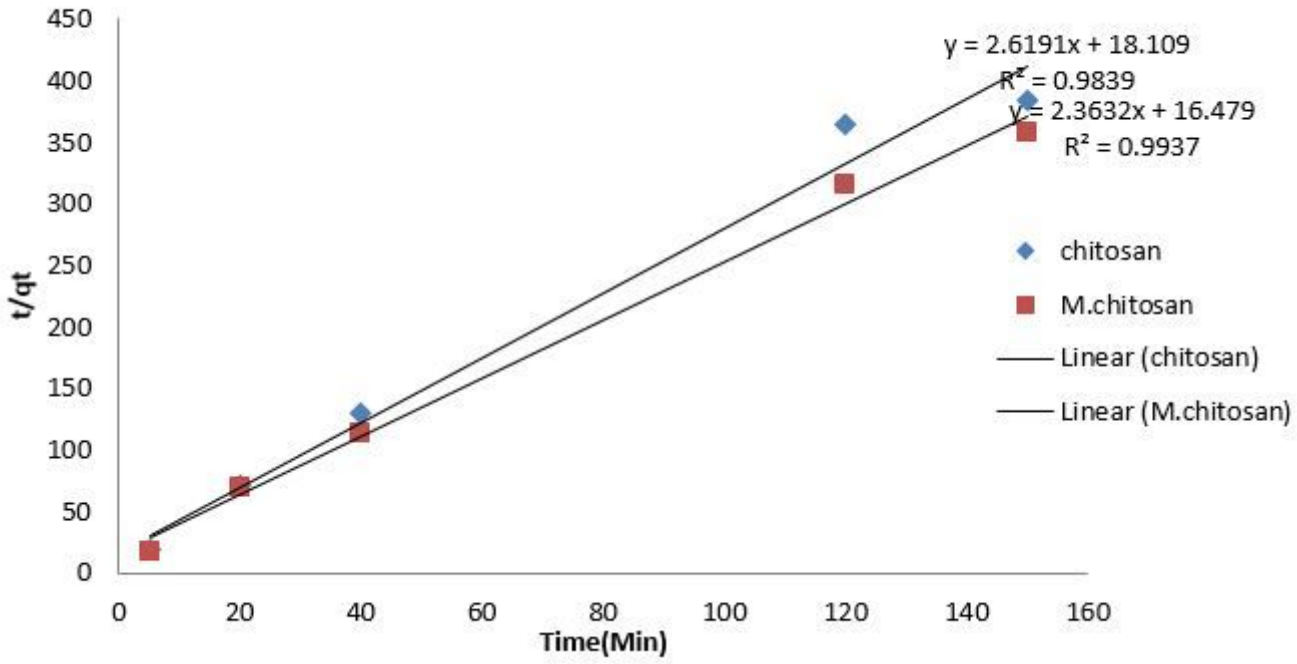

Figure 16

Plot of pseudo-second order kinetics for Pb^{2+} adsorption by extracted chitosan and modified chitosan

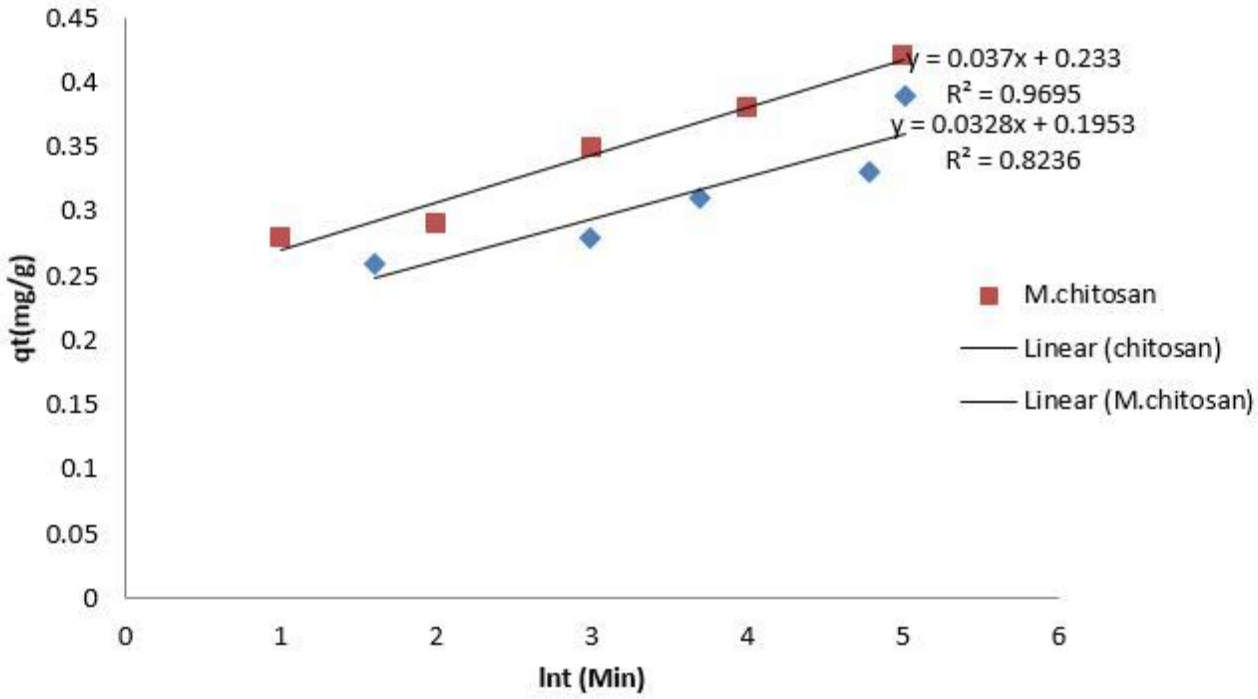

Figure 17

Plot of Elovichkinetics for Pb^{2+}adsorption by extracted chitosan andmodified chitosan.

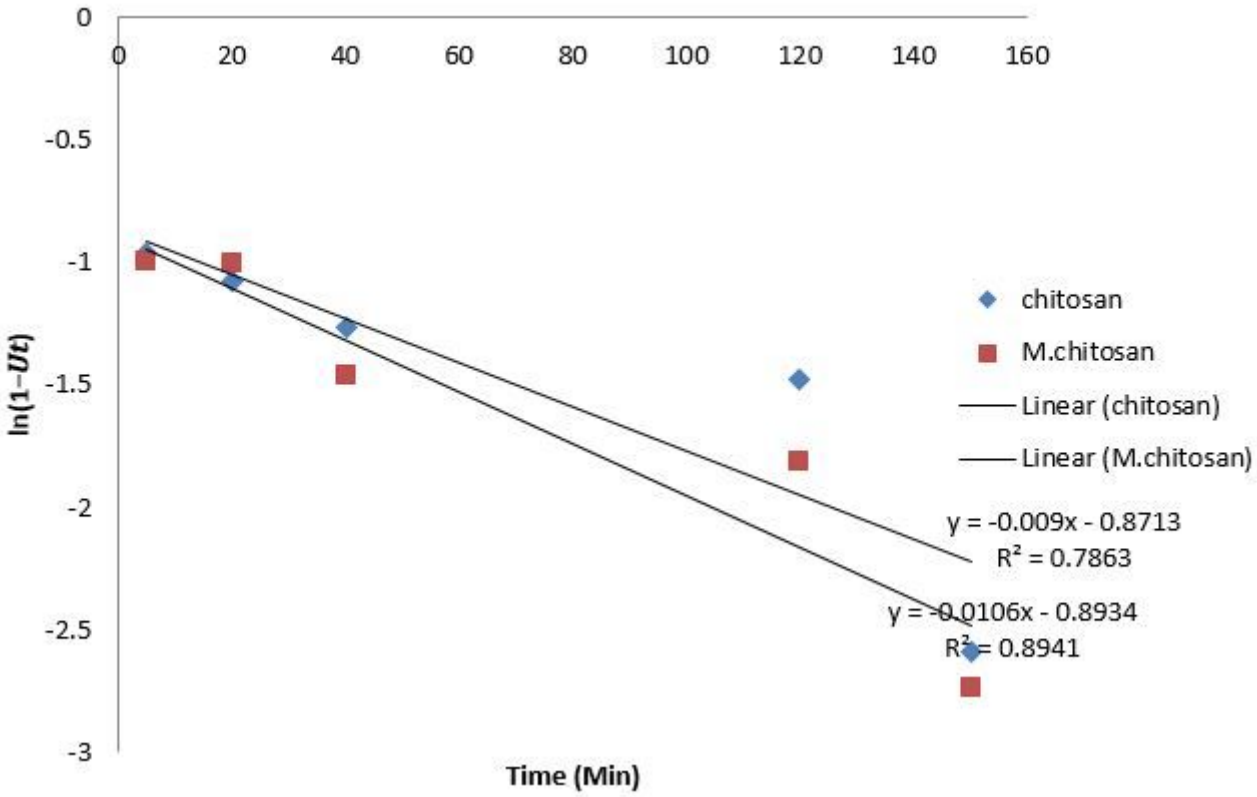

Figure 18

Plot of Bhattacharya and Venkobacharkinetics for Pb^{2+} adsorption by extracted chitosan andmodified chitosan.

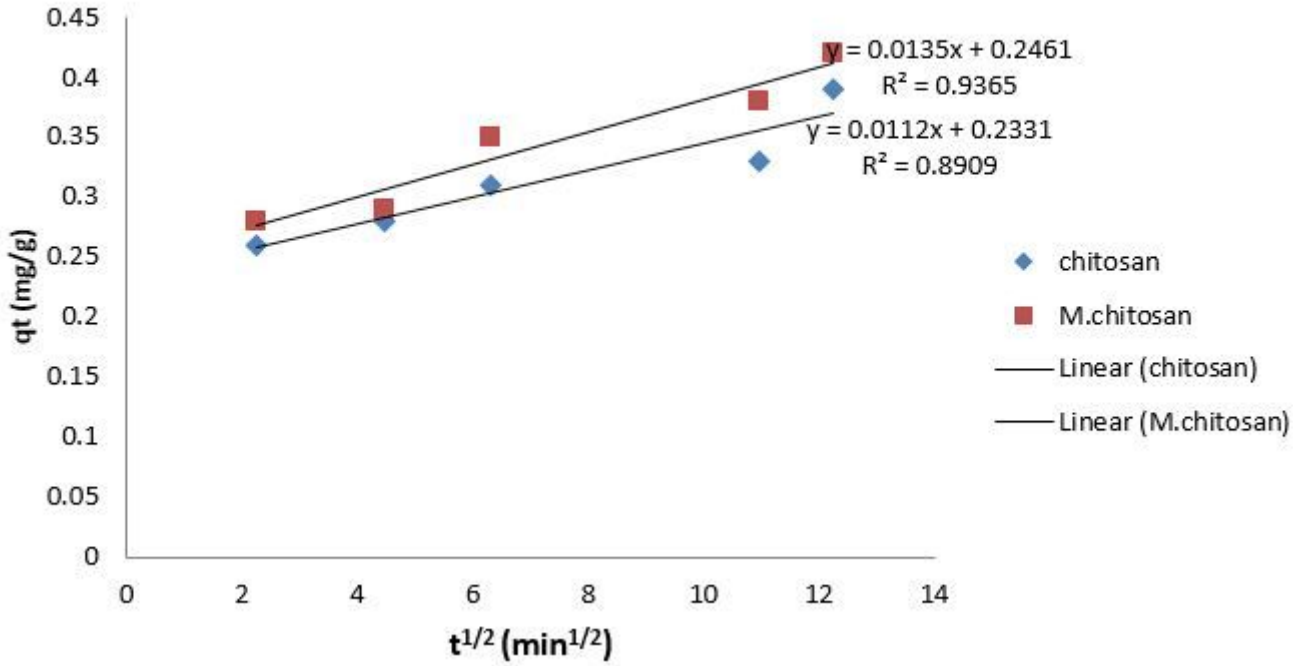

Figure 19

Plot of intra-particle diffusion kinetics for Pb^{2+} adsorption by extracted chitosan and modified chitosan.

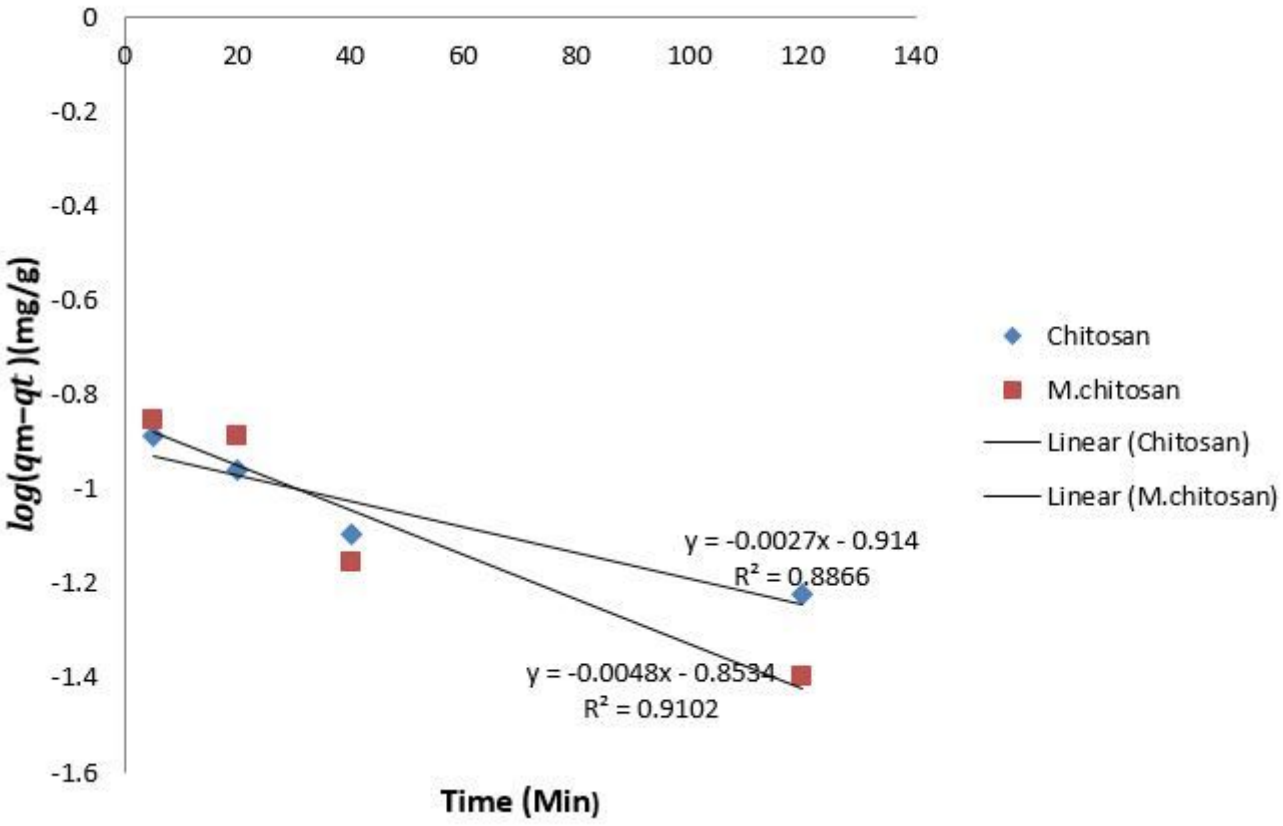

Figure 20

Plot of film diffusion kinetics for Pb^{2+} adsorption by extracted chitosan and modified chitosan.

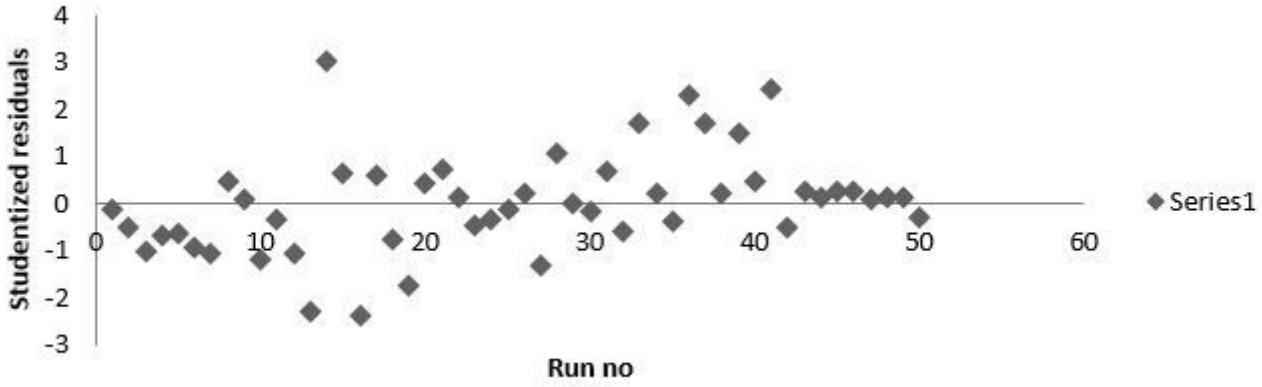

Figure 21

A plot of studentized residuals versus run order